atmosphere

MDPI

Article

A Simple Empirical Method for Estimating Extreme Air Velocities from CFD Mean-Flow Statistics: Validation Using ISS Columbus and CASA Ventilation Data

George Efthimiou [1,2]

[1] FLUENC, 55535 Thessaloniki, Greece; gefthimiou@fluenc.gr or gefthimiou@ipta.demokritos.gr
[2] Environmental Research Laboratory, Institute of Nuclear and Radiological Sciences and Technology, Energy and Safety, National Centre for Scientific Research "Demokritos", 15341 Agia Paraskevi, Greece

Abstract

Computational Fluid Dynamics (CFD) simulations based on Reynolds-Averaged Navier–Stokes (RANS) models are widely used for spacecraft cabin ventilation design; however, they primarily provide mean-flow quantities and often underestimate velocity extremes relevant to crew comfort, ventilation effectiveness, and stagnation-zone assessment. This study presents a simple empirical post-processing framework for estimating extreme air velocities from CFD mean-flow statistics. The proposed approach expresses the upper velocity envelope as a function of the local mean velocity and standard deviation through a single empirical coefficient, Kc. Throughout this study, the upper velocity envelope is defined consistently as the 99th percentile of the velocity magnitude distribution, denoted p99, and the empirical peak factor is accordingly defined as $Kc_{,p99} = (p99 - \mu)/\sigma$. This definition is applied uniformly to the calibration dataset and to all external validation datasets, so that the same target variable is used at every stage of the analysis. The method is calibrated using published velocity-field data from International Space Station (ISS) Crew Quarters studies and subsequently examined against independent ISS ventilation datasets, including the Columbus module and Crew Alternative Sleeping Area (CASA) configurations. Analysis of digitized experimental and CFD-derived velocity distributions yields a robust median coefficient of approximately Kc = 4.5, while external datasets indicate p99-equivalent values generally within the range $Kc \approx 4$–6. Independent validation evidence from Columbus ventilation studies demonstrates that accounting for velocity fluctuations substantially improves agreement with experimental observations, reducing distribution mismatch by approximately 83% compared with uncorrected mean-velocity predictions. The external comparison should be understood as a retrospective consistency check rather than a prospective prediction: the peak factors reported for the Columbus and CASA datasets were derived from the same distributions against which they are compared, and they therefore describe the data rather than forecast it. Accordingly, the proposed framework is presented as an exploratory upper-envelope indicator whose transferability is suggested, but not yet demonstrated, by the observed clustering of independently derived peak factors. The results suggest that a simple statistical correction applied to standard CFD outputs can provide practical estimates of extreme ventilation velocities without the computational cost of Large Eddy Simulation (LES). While the proposed framework should be regarded as an exploratory upper-envelope indicator rather than a universal turbulence closure, and while it does not by itself provide a conservative bound or identify stagnation risk, the consistency observed across multiple ISS ventilation datasets indicates that it offers a useful preliminary screening tool for spacecraft cabin ventilation assessment and design.

Check for updates

Academic Editor: Se-Woon Hong

Received: 8 August 2026
Revised: 5 October 2026
Accepted: 13 October 2026
Published: 16 October 2026

Copyright: © 2026 by the author. Licensee MDPI, Basel, Switzerland. This article is an open access article distributed under the terms and conditions of the Creative Commons Attribution (CC BY) license.

Keywords: CFD; RANS; spacecraft ventilation; ISS; Columbus module; CASA; extreme velocity estimation; airflow distribution; empirical modeling; indoor airflow

1. Introduction

Airflow management is a critical component of Environmental Control and Life Support Systems (ECLSSs) in crewed spacecraft. Unlike terrestrial indoor environments, spacecraft cabins operate under microgravity conditions where buoyancy-driven transport is largely absent and forced ventilation becomes the dominant mechanism governing heat transfer, contaminant removal, carbon dioxide transport, humidity control, and crew thermal comfort [1,2]. Consequently, accurate prediction of cabin airflow patterns has become an essential requirement in spacecraft design and operation [3,4].

Computational Fluid Dynamics (CFD) has become the primary engineering tool for evaluating spacecraft ventilation systems because experimental testing is expensive and often impractical during early design stages [5,6]. Reynolds-Averaged Navier–Stokes (RANS) simulations are particularly attractive because they provide acceptable engineering accuracy at relatively low computational cost compared with higher-fidelity approaches such as Large Eddy Simulation (LES) or Direct Numerical Simulation (DNS) [7,8]. As a result, RANS-based CFD has been extensively applied to spacecraft cabin ventilation studies, including investigations of the International Space Station (ISS), crew quarters, sleeping compartments, and planetary habitat concepts [6,9,10].

Despite their widespread use, conventional RANS simulations primarily provide time-averaged flow quantities. The predicted velocity magnitude is therefore a mean-flow quantity that does not directly represent the instantaneous velocity fluctuations experienced by astronauts [7,8]. This limitation is particularly important when assessing local maximum velocities, draft sensation, airflow discomfort, ventilation effectiveness, or stagnant regions. In practice, many engineering decisions are influenced not by the mean velocity itself but by the upper tail of the velocity distribution [11–13].

The distinction between mean and fluctuating velocities has long been recognized in indoor environmental engineering. Numerous studies have demonstrated that turbulence intensity significantly affects human thermal comfort, perceived air movement, contaminant transport, and local ventilation effectiveness [11–15]. In terrestrial ventilation applications, local velocity distributions are often characterized using statistical quantities such as turbulence intensity, standard deviation, and percentile-based metrics rather than mean velocity alone [13,16]. Similar considerations are expected to apply in spacecraft environments, where ventilation-generated turbulence governs the transport of exhaled contaminants and thermal plumes in the absence of buoyancy-driven mixing [1,2].

Several investigators have therefore examined approaches that incorporate velocity fluctuations into ventilation assessment [9], demonstrating that velocity distributions derived from turbulent statistics produced substantially better agreement with experimental measurements in the Columbus module than distributions based solely on mean velocity. Similar observations have been reported in terrestrial indoor airflow studies, where fluctuation-based metrics consistently outperform mean-flow quantities when comparing CFD predictions with measured velocity distributions [4,14,15]. These findings suggest that a significant portion of the discrepancy between CFD predictions and measured ventilation performance may arise from neglecting velocity variability.

At the same time, obtaining reliable estimates of extreme velocities remains challenging. LES can resolve a substantial fraction of the turbulent energy spectrum and provide direct access to instantaneous flow structures, but its computational requirements

remain prohibitive for routine spacecraft design applications [8,17]. Even in terrestrial building simulations, LES is generally reserved for research investigations rather than engineering practice [4,15]. Consequently, there is continuing interest in methods capable of extracting additional design-relevant information from standard RANS simulations without substantially increasing computational cost.

The limitations of RANS closures in confined flows are well documented. Because RANS formulations solve for time-averaged quantities, they inherently smooth out the instantaneous velocity peaks that govern draft sensation, local heat transfer, and contaminant dispersion. Complementary insights into confined-space airflow have been obtained in other transport environments. Although studies in the literature address terrestrial transport infrastructure rather than crewed spacecraft, they share with the present work the central challenge of characterising turbulent ventilation in geometrically confined, buoyancy-limited environments, and they reinforce the need for simple, computationally inexpensive methods that can estimate velocity extremes from standard CFD outputs.

Extreme-value estimation has a long history in fluid mechanics, atmospheric science, hydrology, reliability engineering, and wind engineering [18–20]. In many applications, maximum values are represented as a function of the mean and a measure of variability, often expressed through statistical exceedance coefficients or peak factors [18,20]. Similar concepts are routinely employed in atmospheric dispersion modeling, wind loading calculations, and environmental risk assessment [21,22]. However, relatively little attention has been devoted to analogous approaches for spacecraft cabin ventilation, particularly for estimating local velocity maxima from CFD-derived flow statistics.

Recent ISS ventilation datasets provide a unique opportunity to examine this problem. Published measurements and CFD results from ISS Crew Quarters, Columbus module investigations, and Crew Alternative Sleeping Area (CASA) studies contain information on velocity distributions, local maxima, and turbulent variability across a range of operational configurations [9,10]. Collectively, these datasets span both experimental and numerical investigations and therefore offer an appropriate foundation for evaluating simple statistical relationships between mean-flow quantities and observed velocity extremes.

The present study investigates whether local extreme air velocities can be estimated using a simple empirical relationship based solely on mean-flow statistics. The proposed formulation expresses the upper velocity envelope as

$$X_{max} = \mu + K_c \sigma \quad (1)$$

where μ is the mean velocity, σ is the velocity standard deviation, and Kc is an empirical coefficient representing the effective distance between the mean state and the extreme portion of the velocity distribution.

Unlike conventional turbulence models, the proposed coefficient is not intended to represent a universal physical closure. Instead, it is treated as an engineering parameter that can be calibrated from published ventilation datasets and subsequently applied as a practical post-processing tool. The central hypothesis of this work is that a relatively narrow range of Kc values characterizes extreme ventilation velocities in spacecraft cabin environments and that this range can be inferred from existing ISS datasets.

To evaluate this hypothesis, velocity-field information digitized from published ISS Crew Quarters studies is used for calibration, while independent Columbus and CASA datasets are employed for validation. Particular emphasis is placed on assessing whether a robust, transferable value of Kc can reproduce reported maximum velocities and percentile-equivalent extremes across multiple spacecraft ventilation configurations. The resulting framework is intended to provide spacecraft ventilation engineers with a simple method for estimating extreme airflow conditions directly from standard RANS outputs, thereby bridg-

ing part of the gap between mean-flow CFD predictions and design-relevant ventilation performance metrics.

The remainder of this paper is organized as follows. Section 2 describes the empirical methodology, including the formulation of the extreme-velocity estimator $X_{max} = \mu + K_c\sigma$, the definition of the calibration coefficient K_c, and the digitization procedure used to extract velocity profile data from published figures. Section 3 presents the three independent ISS ventilation datasets employed in this study: the Crew Quarters experimental and CFD data from [10], the Columbus module RANS/LES/experimental comparison from [23], and the Crew Alternative Sleeping Area (CASA) velocity distribution studies from 2022 and 2023. Section 4 reports the calibration results for K_c, the leave-one-out cross-validation (LOOCV) performance, and the error metrics (MAE, RMSE, relative error) across all datasets. Section 5 discusses the physical interpretation of the results, compares the proposed approach with existing RANS correction methods (e.g., the $V_a = \sqrt{V_m^2 + \frac{5}{3}k}$ formulation), and acknowledges the limitations of figure-derived data. Finally, Section 6 summarizes the main conclusions and outlines practical recommendations for applying the empirical framework in spacecraft cabin ventilation design and preliminary assessment.

2. Methodology

2.1. Theoretical Framework & Peak Velocity Estimation

To predict localized peak velocity magnitudes (U_{max}) within microgravity cabin environments using time-averaged Reynolds-Averaged Navier–Stokes (RANS) simulations, an empirical post-processing model is employed:

$$U_{max} = \mu + K_c\sigma \tag{2}$$

Definition of the target extreme. The estimator expressed by Equation (2) requires a precise definition of the extreme velocity Umax. In the present work, Umax is identified with the 99th percentile of the velocity magnitude distribution, p99, evaluated over the same sampling domain and with the same spatial resolution for every dataset considered. The 99th percentile is preferred over the absolute maximum because the latter depends on the number of samples, the spatial resolution, the sampling frequency, and the autocorrelation of the velocity signal, and is therefore not a reproducible target across datasets with different reporting formats. The peak factor is consequently defined as

$$Kc,p99 = (p99 - \mu)/\sigma$$

and this definition is maintained throughout the calibration and validation. Where published datasets report only grouped velocity distributions or figure-derived profiles, p99 is estimated by interpolation of the reported cumulative distribution, as described in Section 2.4.

In the model:

- μ is the spatial or time-averaged mean velocity magnitude (m/s).
- σ is the velocity standard deviation (m/s), representing turbulent velocity fluctuations. In standard RANS turbulence models (e.g., $k - \varepsilon$ or $k - \omega$ SST), assuming local isotropic turbulence, σ is estimated from the turbulent kinetic energy k as:

$$\sigma = \sqrt{\frac{2}{3}k} \tag{3}$$

It must be emphasised that Equation (3) provides an order-of-magnitude estimate of the velocity variability rather than an exact expression for the standard deviation of the

velocity magnitude $|\mathbf{U}|$. Under the local-isotropy assumption, $\sqrt{\frac{2}{3}k}$ represents the RMS fluctuation of a single velocity component, not the standard deviation of the composite magnitude. Relating the two quantities requires additional assumptions about the joint probability distribution of the three velocity components. If the components are assumed to be independent, zero-mean, and Gaussian with equal variance $2k/3$, then the variance of the magnitude can be approximated by propagating the component variances; in the limit of small turbulence intensity relative to the mean speed, this yields $\sigma|U| \approx \sigma ui'$, which is the approximation implicitly adopted here. This approximation degrades as the local mean velocity approaches zero, where the magnitude becomes a strictly positive quantity dominated by the fluctuating part and the linear decomposition $|U| \approx \mu + Kc$ loses its physical basis. In such low-mean-velocity regions—for example stagnation zones and the cores of recirculation cells—the present formulation should be regarded as a heuristic envelope indicator rather than a calibrated statistical predictor. The empirical coefficient Kc introduced below therefore absorbs not only the ratio between the extreme and the standard deviation of the magnitude, but also the residual error introduced by using Equation (3) as a surrogate for $\sigma|U|$. This is consistent with the explicitly empirical character of the proposed framework and with its intended use as a post-processing screening tool for standard RANS outputs.

- K_c is the dimensionless peak multiplier factor (coverage factor), reflecting the extreme deviations of the velocity field from the mean state driven by turbulent fluctuations and flow non-uniformities.

By rearranging the governing expression, the empirical peak factor for any given profile or dataset is calibrated as:

$$K_c = \frac{U_{max} - \mu}{\sigma} \tag{4}$$

It is emphasized that Kc is not a conservative safety factor in a probabilistic sense. The leave-one-out cross-validation results presented in Section 4.2 show that the combined median Kc = 4.47 can underpredict the highest CFD-predicted maxima. Therefore, Kc should be interpreted as an empirical envelope indicator, not as a guaranteed upper bound. In addition, because the estimator targets the upper tail of the velocity distribution, it is not suitable for identifying stagnation risk, which is controlled by the lower tail.

An important distinction must be made between the temporal and spatial interpretations of σ in Equation (2). In the theoretical formulation, σ represents the local temporal standard deviation of turbulent velocity fluctuations at a fixed point, approximated from the turbulent kinetic energy k via Equation (3). In the calibration procedure described in Section 2.2, however, μ and σ are computed over thousands of spatially distributed points within a digitised cross-sectional plane. In that context, σ quantifies spatial heterogeneity between jet cores, wall-adjacent regions, and low-velocity zones, rather than temporal turbulence at a single location. Unless a functional relationship between the spatial standard deviation σs and the temporal turbulent standard deviation σt is established, the two quantities are not interchangeable. The empirical coefficient Kc calibrated from spatially distributed data therefore represents an **upper spatial envelope estimator**, not a local temporal extreme estimator. This distinction is maintained throughout the manuscript, and its implications for the interpretation of Kc are discussed further in Section 5.1.

2.2. Primary Dataset Digitization & Calibration (Dataset from [10])

Calibration of K_c was performed using experimental Particle Image Velocimetry (PIV) and RANS Computational Fluid Dynamics (CFD) velocity profiles published in [10] across five cross-sectional measurement planes (P1 through P5) in an ISS module cabin mock-up.

2.2.1. Digitization Protocol

Because raw numerical data were unavailable, spatial velocity distribution curves were extracted from high-resolution figure panels using WebPlotDigitizer (https://apps.automeris.io/wpd/, accessed on 12 October 2026):

1. **Coordinate system calibration:** Axis limits (V_{min},V_{max}) and spatial coordinates were mapped across plane panels.
2. **Data sampling:** Continuous spatial profiles were digitized at high density (n ≈ 1000–3600 points per plane).
3. **Statistical extraction:** Spatial mean (μ), spatial standard deviation (σ), and the 99th percentile of the velocity magnitude distribution were computed for each plane and source. The printed maximum velocity reported in the original figure is also recorded for reference, but it is not used as the calibration target, because a printed maximum and a 99th percentile are not equivalent quantities and cannot be compared directly across datasets with different sampling characteristics.

It is emphasised that the spatial mean (μ) and spatial standard deviation (σ) extracted through this protocol are spatial statistics computed over a two-dimensional cross-section. They characterise the heterogeneity of the velocity field across the measurement plane and are not equivalent to the temporal mean and temporal standard deviation that would be obtained from time-resolved measurements at a single point. Consequently, the peak factor Kc derived from these statistics should be interpreted as a spatial upper-envelope multiplier rather than a temporal turbulence closure coefficient. This interpretation is consistent with the engineering purpose of the proposed method, which is to provide a preliminary estimate of the upper tail of the velocity distribution across cabin cross-sections using standard RANS outputs.

2.2.2. Calibration Results

Individual plane peak factors ($K_{c,fit}$) were determined for all 10 plane/source combinations. To establish a generalized parameter for spacecraft cabin ventilation, robust central tendency statistics were evaluated:

- **Combined median:** K_c = 4.47.
- **PIV sub-group median:** $K_{c,PIV}$ = 4.12.
- **CFD Sub-group median:** $K_{c,CFD}$ = 6.11.

2.3. Cross-Validation Scheme (Leave-One-Plane-Out CV)

The calibration dataset consists of five physical measurement planes (P1–P5) of the Crew Quarters study [10], each represented by two velocity profiles: one from Particle Image Velocimetry (PIV) and one from RANS CFD. These ten profiles therefore do not constitute ten independent physical configurations. Instead, they represent five independent flow-field realisations, each sampled by two different techniques. The large number of digitised points per profile (approximately 1000–3600) increases the spatial resolution of each realisation but does not increase the number of statistically independent physical cases.

To avoid information leakage between training and test data, a Leave-One-Plane-Out Cross-Validation (LOPO-CV) scheme was adopted instead of the conventional Leave-One-Out scheme. For each iteration i (where i = 1, . . ., 5 indexes the measurement planes):

1. Both the PIV and the CFD profile of plane i were removed from the training set.
2. The robust median peak factor $K_{c,train}^{(-i)}$ was computed from the remaining eight profiles (four planes × two sources).
3. The peak velocity for each held-out profile j (PIV and CFD of plane i) was predicted as

$$\hat{U}_{max,j} = \mu_j + K_{c,train}^{(-i)} \cdot \sigma_j \quad (5)$$

4. Model error was evaluated using Mean Absolute Error (MAE), Root Mean Square Error (RMSE), Mean Bias (Bias), and Mean Absolute Percentage Error (MAPE).

Because the held-out PIV and CFD profiles originate from the same physical plane, they share the same mean-flow structure and are therefore not independent of each other. This shared dependence is retained deliberately: it reflects the realistic engineering situation in which a single plane is characterised by two measurement techniques and allows the framework to be tested under the worst-case assumption that no independent plane is available. For a stricter test that also removes the shared plane dependence, the leave-one-configuration-out scheme discussed in Section 5.7 would be required.

It should be emphasised that the number of independent physical cases in the calibration dataset is five, not ten. All error metrics reported in Section 4.2 are therefore based on a small sample, and the resulting confidence intervals are correspondingly wide. This limitation is inherent to the available published data and is acknowledged explicitly in Section 5.4. Any recommendation derived from this calibration should be treated as preliminary and subject to re-calibration when additional independent datasets become available.

2.4. External Dataset Processing & Velocity Component Correction

The generalizability of K_c was validated against independent spacecraft cabin datasets:

- **Columbus module benchmark:** Dataset from [23] (6 cases covering RANS, LES, and experimental measurements).
- **Crew Alternate Sleeping Accommodation (CASA) benchmarks:** Datasets from [24,25] across different ventilation flow rates (27 CFM baseline vs. improved plenum configurations).

2.4.1. 3D Velocity Magnitude Adjustment ($\mathbf{V_m}$ to $\mathbf{V_a}$)

In cabin ventilation studies, reporting single-component or planar mean velocities (V_m) underestimates true 3D flow speeds (V_a), leading to artificial inflation of requirement non-compliance. A distribution-level conversion was applied to reconstruct true magnitude statistics (μ_{3D}, σ_{3D}) from component distributions:

- **Component velocity** (V_m): Raw spatial mean velocity magnitude in 2D measurement planes.
- **3D corrected velocity** (V_a): Full vector velocity magnitude accounting for 3D turbulence isotropy and spatial variance.

The efficacy of V_a correction was measured by comparing distribution error reductions against experimental benchmarks:

$$\text{Error Reduction } (\%) = \left(1 - \frac{\text{MAE}(V_a)}{\text{MAE}(V_m)}\right) \times 100\% \quad (6)$$

2.4.2. 99th Percentile Equivalent $\mathbf{K_c}$ ($\mathbf{K_{c,p99}}$)

For external datasets where absolute maximums represent spatial outliers, the 99th percentile velocity ($p99$) was selected as a robust proxy for maximum operational cabin airspeed. The equivalent coverage factor was calculated as:

$$K_{c,p99} = \frac{p99 - \mu}{\sigma} \quad (7)$$

Consistency of the target extreme across datasets. Equation (7) defines the same target variable that is used for the calibration in Section 2.2, namely the 99th percentile of the velocity magnitude distribution normalised by the local mean and standard deviation. The use of p99 for the external datasets is therefore not an ad hoc substitute for an unavailable maximum; it is the common metric adopted throughout this study. The printed maxima reported in the original publications are retained only as descriptive quantities and are not used in any quantitative comparison with the calibrated Kc values.

2.4.3. Ventilation Compliance Evaluation

Predicted velocity distributions were evaluated against standard NASA ISS cabin ventilation specifications:

- **Stagnant/low-velocity threshold:** $U < 0.051$ m/s (10 ft/min)
- **Target airspeed window:** $0.051 \text{ m/s} \leq U \leq 0.203$ m/s ($10 - 40$ ft/min)
- **Draft/high-velocity threshold:** $U > 0.203$ m/s (40 ft/min)

Throughout this study, the ISS target ventilation window is defined as 0.051–0.203 m/s (10–40 ft/min), and stagnant conditions are defined as $U < 0.051$ m/s (10 ft/min). All subsequent analyses use this common definition. Where the original source studies adopted a different lower threshold (e.g., 0.051 m/s, 15 ft/min), that threshold is explicitly identified and the data are re-evaluated against the common 10 ft/min criterion for comparability.

2.5. Use of Generative AI in Data Digitization

Generative AI was used in this study solely as a technical aid for extracting numerical data from published figures. Specifically, GPT-6 of OpenAI was used to assist in digitizing selected published plots. The tool was used to convert graphical data points from published images into numerical values for subsequent statistical analysis. All AI-assisted extractions were reviewed and verified against the original published figures. The AI tool was not used to generate new data, perform statistical calculations, interpret results, or draft the scientific content. The author takes full responsibility for the accuracy and interpretation of all data.

3. Data Sources

To calibrate and validate the proposed empirical extreme-velocity estimator, three independent datasets from published ISS ventilation studies were employed. These cover different cabin geometries, ventilation configurations, and measurement techniques, providing a robust basis for assessing the generality of the present method.

3.1. Crew Quarters [10]

The primary calibration dataset was obtained from the experimental and numerical investigation of the ISS Crew Quarters (CQ) ventilation system in [10]. That study provided detailed velocity fields from both Particle Image Velocimetry (PIV) measurements in a 1:4 scale water model and full-scale RANS CFD simulations (realizable k-ε model) of the isothermal airflow inside the CQ cabin.

Five vertical measurement planes (P1–P5) were defined across the CQ interior, covering the region from the supply diffuser to the exhaust grille. For each plane, spatial distributions of the velocity magnitude were reported. From these, the present work extracted:

- The spatial mean velocity, μ;
- The spatial standard deviation, σ;
- The 5th and 95th percentiles, p05 and p95;
- The 99th percentile of the velocity magnitude distribution, p99, used as the common extreme metric throughout this study;
- The printed local maximum velocity, Umax, recorded for reference only.

A total of ten independent profiles were digitised (five planes × two sources—PIV and CFD) using WebPlotDigitizer, with sampling densities ranging from approximately 1000 to 3600 points per profile. From each profile, the spatial mean, spatial standard deviation, and 99th percentile were extracted, and the plane-specific peak factor was computed as $Kc,p99 = (p99 - \mu)/\sigma$. This dataset was used to derive the initial calibration of the peak factor Kc, as described in Section 2.2.

3.2. Columbus Module [23]

The first independent validation dataset comes from the benchmark study of Columbus module ventilation [23]. That work compared RANS and Large Eddy Simulation (LES) predictions with experimental velocity measurements obtained using omnidirectional thermal anemometers at 25 monitoring points within the module.

Three computational cases were considered:

- Case 1: RANS with uniform inlet velocity distribution across all diffuser slits;
- Case 2: RANS with non-uniform slit widths and flow angles as per the experimental diffuser settings;
- Case 3: LES with the same detailed inlet conditions as Case 2.

For each case, both the mean velocity magnitude ($V_m = |\langle \mathbf{V} \rangle|$) and the time-averaged speed ($V_a = \langle |\mathbf{V}| \rangle$) were reported. The experimental data correspond to Va, since the probes were insensitive to flow direction. In the present study, the RANS Case 2 data (i.e., the mean velocity field and turbulent kinetic energy k are used to test the proposed Kc-based correction, while the LES and experimental results serve as reference truths for evaluating the accuracy of the estimated extremes.

3.3. Crew Alternative Sleeping Area—CASA [24,25]

The second independent validation dataset concerns the Crew Alternative Sleeping Accommodation (CASA), a sleeping compartment installed in the Columbus module. Two successive CFD studies [24,25] examined the airflow distribution inside CASA using URANS (realizable k-ε) simulations with polyhedral meshes (≈5.6 million cells) and included a detailed crewmember model (ECLOID) in standing or sleeping positions.

From the 2022 study [24], the baseline ventilation scenario with a supply flow rate of 27 ft^3/min (0.76 m^3/min) was used. Velocity magnitude data were extracted from 23 cross-sectional planes (five in the X-direction, eleven in Y, seven in Z). The 2023 study [25] examined an improved exhaust plenum configuration with additional return grilles and floor filters, and also provided carbon dioxide distribution data. For the present work, only the velocity fields from the baseline (2022) and modified plenum (2023, Case 3 with 27 ft^3/min and porous-jump resistance) configurations are considered.

As in the Columbus study, the RANS-computed mean velocity Vm and turbulent kinetic energy k are used to evaluate the empirical estimator. The reported velocity distributions—expressed as percentages of cabin volume falling into specified velocity

bands (e.g., 10–40 ft/min)—are used to derive equivalent p99 values and to compute the corresponding Kc,p99 factors, following the procedure outlined in Section 2.4.

3.4. Summary of Dataset Usage

All velocity data were converted to consistent SI units (m/s) prior to analysis, and the 99th percentile was used as a robust proxy for extreme velocities when absolute maxima were not explicitly reported.

Table 1 presents a summary of ISS ventilation datasets employed in the present study, indicating the source reference, dataset type, and specific role of each dataset in the calibration or validation of the proposed empirical extreme-velocity estimator.

Table 1. Summary of ISS ventilation datasets employed in the present study, indicating the source reference, dataset type, and specific role of each dataset in the calibration or validation of the proposed empirical extreme-velocity estimator.

Dataset	Source	Type	Role in This Study
Crew quarters	[10]	PIV + RANS	Calibration of Kc
Columbus module	[23]	RANS, LES, Experiments	Validation of Kc—comparison with LES/experimental Va
CASA (2022)	[24]	URANS	Validation—velocity band distributions
CASA (2023)	[25]	URANS	Validation—improved plenum configuration

4. Results

4.1. Calibration of the Peak Factor (Kc) from Crew Quarters Data [10]

The empirical coefficient Kc was calibrated using velocity-field statistics digitised from the ISS Crew Quarters study [10]. A total of ten independent profiles were extracted, comprising five PIV measurement planes (P1–P5) and five corresponding RANS CFD planes. For each profile, the spatial mean velocity μ, the spatial standard deviation σ, and the 99th percentile p99 were used to compute the individual plane peak factor as $Kc,p99 = (p99 - \mu)/\sigma$. The use of p99 rather than the printed maximum ensures that the calibration target is identical to the target used for the external datasets and is not sensitive to the number of digitised samples or to the spatial resolution of the original figure.

Table 2 summarises the individual Kc estimates for each plane and source, together with the corresponding mean velocity, standard deviation, and reported maximum.

Table 2. Individual K_c estimates from digitised profiles in [10], showing for each plane and source the spatial mean velocity μ, standard deviation σ, reported maximum velocity U_{max}, and the fitted peak factor $K_c = (U_{max} - \mu)/\sigma$.

Plane	Source	μ (m/s)	σ (m/s)	U_{max} (m/s)	K_c
P1	PIV	0.0561	0.0462	0.1500	2.03
P1	CFD	0.2189	0.1393	0.6400	3.02
P2	PIV	0.0439	0.0460	0.2300	4.05
P2	CFD	0.1918	0.1945	1.3800	6.11
P3	PIV	0.0566	0.0445	0.2400	4.12
P3	CFD	0.2303	0.1871	1.6700	7.69
P4	PIV	0.0557	0.0439	0.4000	7.84
P4	CFD	0.2537	0.1536	1.6500	9.09
P5	PIV	0.0432	0.0429	0.2500	4.82
P5	CFD	0.1771	0.1738	0.8900	4.10

The distribution of Kc values exhibited notable variation between experimental and numerical sources. The PIV-derived coefficients ranged from 2.03 to 7.84 with a median of Kc, PIV = 4.12, while the CFD-derived coefficients ranged from 3.02 to 9.09 with a median of Kc, CFD = 6.11. The combined dataset (PIV + CFD) yielded a median coefficient of Kc = 4.47, with a mean of 5.29 and a range of 2.03–9.09.

Figure 1 presents the distribution of Kc values grouped by source type, highlighting the median values for PIV, CFD, and the combined dataset.

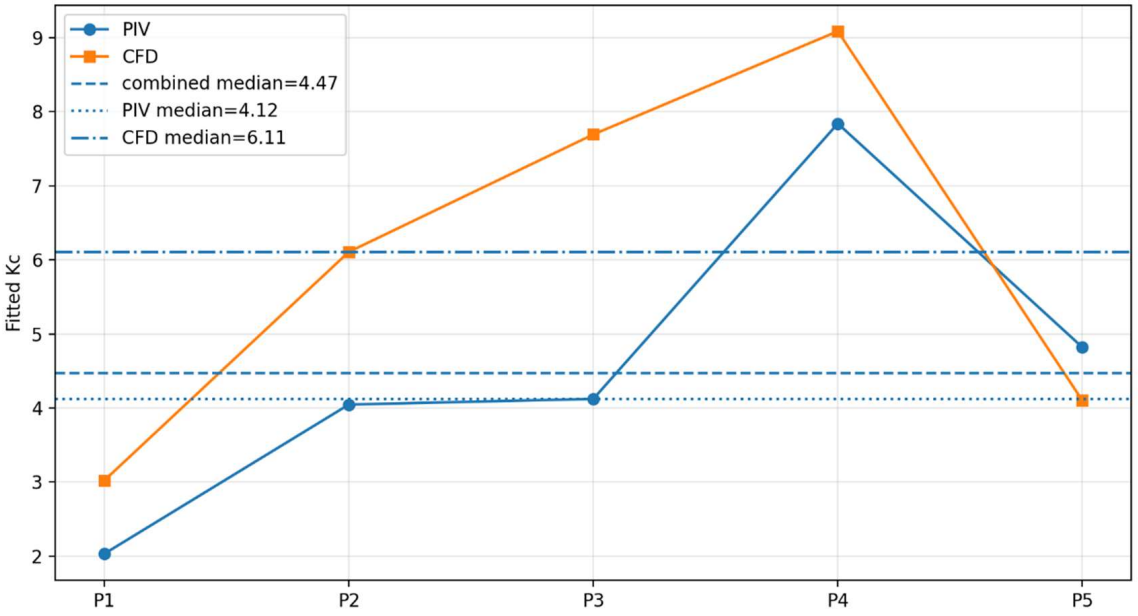


Figure 1. Distribution of Kc values grouped by source type, highlighting the median values for PIV, CFD, and the combined dataset.

To quantify the uncertainty associated with the figure-digitisation process, a Monte Carlo uncertainty analysis was performed assuming ±5% error in μ and Umax and ±10% error in σ. The combined median Kc remained stable at approximately 4.7 (95% CI: 4.11–5.43), confirming that the calibration is not unduly sensitive to digitisation artefacts (Table 3).

Table 3. Bootstrap 95% confidence intervals and Monte Carlo uncertainty estimates for median Kc.

Group	n	Kc,est	Bootstrap CI95,low	Bootstrap CI95,high	Monte Carlo Mean	Monte Carlo CI95,low	Monte Carlo CI95,high
Combined	10	4.47	3.56	7.69	4.72	4.11	5.43
PIV	5	4.12	2.03	7.84	4.31	3.63	5.11
CFD	5	6.11	3.02	9.09	6.13	4.93	7.51

4.2. Internal Predictive Performance: Leave-One-Plane-Out Cross-Validation

The predictive capability of the proposed estimator was evaluated using Leave-One-Plane-Out Cross-Validation (LOPO-CV) on the five Georgescu measurement planes. For each iteration, both the PIV and CFD profiles of the held-out plane were predicted using the median Kc calculated from the remaining eight profiles, and the error metrics were computed against the corresponding reported 99th-percentile velocity p99. As discussed in Section 2.3, the five planes constitute the effective number of independent physical cases; the two profiles per plane are treated as paired observations rather than as independent samples.

Table 4 presents the LOOCV performance metrics using the combined median coefficient Kc = 4.47.

Table 4. Leave-one-plane-out cross-validation performance using the combined median Kc = 4.47. Each held-out plane contributes two paired profiles (PIV and CFD), giving n = 10 predictions across five independent planes.

Scheme	MAE (m/s)	RMSE (m/s)	Bias (m/s)	MAPE (%)	n
Combined median	0.258	0.361	0.056	33.46	10

When source-specific median coefficients were used (PIV: Kc = 4.12; CFD: Kc = 6.11), the performance improved marginally in terms of MAE and RMSE, though the bias and MAPE increased (Table 5). Because only five independent planes are available, the difference between the combined median and source-specific schemes should not be overinterpreted; the two schemes differ by less than the width of the bootstrap confidence intervals reported in Table 3.

Table 5. Leave-one-plane-out cross-validation performance using source-specific median Kc values (PIV: Kc = 4.12; CFD: Kc = 6.11). The source-specific coefficients are computed from the training planes only, so that the held-out plane is never used to estimate the coefficient applied to it.

Scheme	MAE (m/s)	RMSE (m/s)	Bias (m/s)	MAPE (%)	n
Source median	0.251	0.344	0.1057	35.15	10

The bias of 0.1057 m/s is larger in magnitude than the combined median bias of 0.056 m/s, consistent with the increased MAPE.

Figure 2 compares the LOOCV-predicted Umax values against the reported/printed maxima for the combined median scheme.

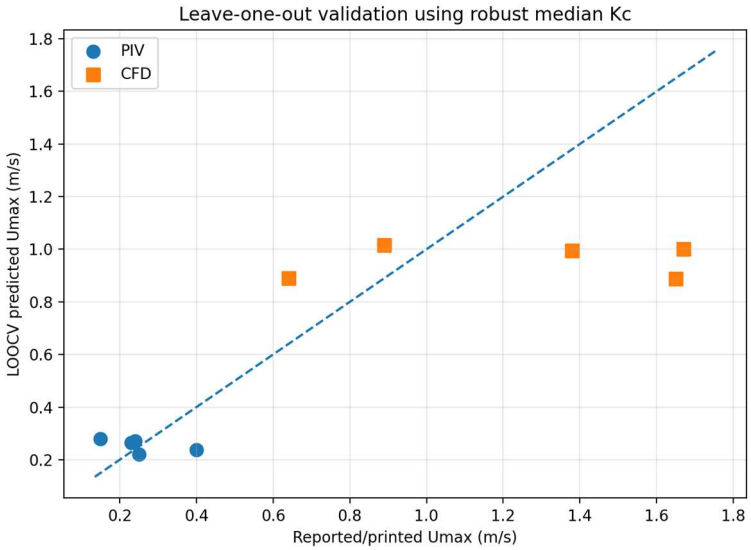


Figure 2. LOOCV predicted vs. observed Umax: scatter plot with 1:1 line.

The LOOCV results indicate that the model performs as a conservative upper-envelope estimator rather than a precise point predictor. These results are based on five independent planes and should therefore be regarded as indicative rather than definitive. The systematic underprediction of the most extreme CFD peaks nonetheless suggests that a single combined median Kc is not sufficient to bound the upper tail of RANS-predicted velocity

distributions, consistent with the interpretation of Kc as an exploratory envelope indicator rather than a conservative design margin.

To interpret these error metrics in a design context, it is necessary to distinguish between the accuracy required for preliminary screening and that required for detailed design verification. The MAE of 0.258 m/s and MAPE of 33.5% obtained with the combined median coefficient are large in relative terms. However, they should be evaluated against the narrow velocity range that characterizes spacecraft cabin ventilation. The ISS target band spans only 0.152 m/s (0.051–0.203 m/s), so an absolute error of 0.258 m/s exceeds the width of the entire acceptable operating window. This means that the estimator cannot, by itself, determine whether a specific location complies with the ventilation specification; it can only indicate whether a location is likely to fall in the low-, target-, or high-velocity regime. For preliminary screening, this level of discrimination is often sufficient, because the purpose is to identify regions that warrant further investigation rather than to certify compliance. For detailed design verification, where the goal is to demonstrate that all occupied volumes fall within the required band, the estimator should be supplemented by higher-fidelity methods or by direct experimental validation. The distinction is therefore not between an acceptable and an unacceptable error, but between an error that is tolerable for the intended screening use and one that is not. The recommended Kc values in Tables 11 and 13 should be applied with this distinction in mind. A more conservative coefficient (e.g., Kc = 6.1, the CFD-derived median) reduces the risk of underpredicting extreme velocities at the cost of overpredicting them in low-variability regions, whereas the combined median (Kc = 4.47) provides a more balanced error profile across the full dataset. Neither choice eliminates the need for follow-up analysis in regions identified as critical.

4.3. Comparison of Fixed Kc Rules

To identify the optimal fixed coefficient for practical application, several candidate Kc rules were evaluated against the calibration dataset. Table 6 summarises the error metrics for each rule.

Table 6. Performance of candidate fixed Kc rules on Georgescu calibration data.

Calibration Group	Kc Rule	Kc	MAE (m/s)	RMSE (m/s)	Bias (m/s)	MAPE (%)
Combined	L2_RMSE_opt	6.04	0.204	0.258	0.030	39.10
Combined	median_L1_robust	4.47	0.221	0.324	−0.138	27.41
Combined	Mean	5.29	0.211	0.274	−0.050	32.92
Combined	fixed_4	4.00	0.234	0.362	−0.189	26.19
PIV	L2_RMSE_opt	4.50	0.062	0.084	−0.002	26.90
PIV	median_L1_robust	4.12	0.059	0.086	−0.019	23.76
CFD	L2_RMSE_opt	6.15	0.308	0.347	0.011	30.63
CFD	median_L1_robust	6.11	0.307	0.348	0.005	30.37
CFD	fixed_4	4.00	0.407	0.505	−0.353	28.36

The L2-optimal coefficient for the combined dataset, Kc = 6.04, produced the lowest MAE and RMSE but the highest MAPE. In contrast, the robust median coefficient Kc = 4.47 yielded lower MAPE (27.4%) and a modest negative bias, consistent with its role as a conservative estimator. The fixed value Kc = 4 produced similar MAPE to the median but larger RMSE and bias, suggesting that Kc values in the range 4–6 are defensible for practical application.

4.4. External Validation: Columbus Module Dataset [23]

In this section and in Section 4.5, the external datasets are evaluated using the same target variable that was used for calibration, namely the 99th percentile of the velocity magnitude distribution. The peak factors reported for the Columbus and CASA datasets are therefore directly comparable with the calibration values, and no conversion between different extreme metrics is required.

The first independent validation was conducted using the Columbus module benchmark study of [23]. This dataset compares RANS predictions, LES results, and experimental measurements at 25 monitoring points, providing both the planar mean velocity Vm and the time-averaged absolute velocity Va.

Table 7 reports the mean absolute percentage error (MAE) between each computational case and the experimental measurements, comparing predictions based on Vm versus Va.

Table 7. Distribution error comparison for Columbus dataset [23]: Vm vs. Va.

Case	Domain	Quantity	MAE to Experiment (%)	L1 (%)	Within-Req Delta (%)	Stagnant Delta (%)
Case 1	whole interior	Vm	27.55	110.20	−52.10	19.30
Case 1	whole interior	Va	8.70	34.80	−17.40	3.00
Case 2	whole interior	Vm	24.75	99.00	−47.10	17.60
Case 2	whole interior	Va	3.40	13.60	−6.80	1.00
Case 2	experimental points	Vm	22.25	89.00	−42.20	13.70
Case 2	experimental points	Va	3.60	14.40	2.70	0.00
Case 3 LES	whole interior	Vm	23.25	93.00	−43.70	13.50
Case 3 LES	whole interior	Va	4.05	16.20	−7.50	0.90
Case 3 LES	experimental points	Vm	22.30	89.20	−44.30	7.10
Case 3 LES	experimental points	Va	0.90	3.60	−1.50	0.00

The uncorrected mean-velocity predictions Vm exhibited substantial errors relative to the experimental distributions, with MAE values ranging from 22.3% to 27.6%. After correction to Va, the MAE was reduced dramatically to between 0.9% and 8.7%. Across all cases, the mean MAE decreased from 24.0% to 4.1%, representing an improvement of 82.8% (Figure 3). It should be emphasised that this 82.8% reduction is obtained by replacing the mean velocity magnitude Vm with the turbulence-augmented velocity Va from [23]. It therefore quantifies the benefit of incorporating turbulent kinetic energy into the velocity magnitude and does not, by itself, constitute a direct validation of the Kc-based estimator proposed in this study.

The improvements were most pronounced for the "within-requirement" velocity band (0.051–0.203 m/s), where Vm predictions underestimated the experimental proportion by 42–52 percentage points, while Va predictions reduced this underestimation to 1.5–17.4 percentage points. Similarly, the overestimation of stagnant zones (<0.051 m/s) was substantially reduced.

Table 8 presents the equivalent coverage factors for the 99th percentile of the Va distributions from the Columbus dataset.

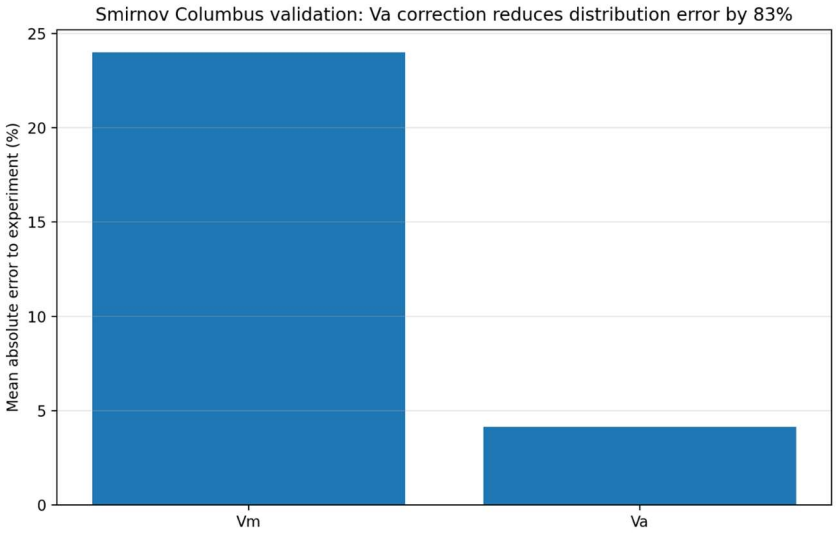


Figure 3. Mean absolute error comparison between Vm and Va for Columbus dataset [23]: bar chart showing 24.0% for Vm and 4.1% for Va.

Table 8. Kc, values derived from Columbus Va distributions [23].

Case	Domain	μ (m/s)	σ (m/s)	p99 (m/s)	Kc,p99
Case 1	whole interior	0.153	0.161	0.918	4.76
Case 2	whole interior	0.164	0.159	0.920	4.76
Case 2	experimental points	0.187	0.175	0.944	4.34
Case 3 LES	whole interior	0.150	0.140	0.885	5.25
Case 3 LES	experimental points	0.169	0.158	0.921	4.77
Experiment	experimental points	0.160	0.143	0.896	5.16

The median Kc,p99 across the Columbus cases was 4.77 (range: 4.34–5.25), which falls within the range established from the Georgescu calibration. Because the same target variable is used in both cases, this comparison is meaningful in a way that a comparison between a printed maximum and a 99th percentile would not be. It must be emphasised that these Kc,p99 values are obtained by normalising the observed 99th-percentile velocity by the observed mean and standard deviation of the same distribution. They therefore constitute a retrospective characterisation of the Columbus velocity fields rather than an independent prediction of their extremes. Their consistency with the calibration range indicates that a peak factor of comparable magnitude emerges across different flow configurations; it does not, by itself, establish the predictive accuracy of the estimator. A prospective test in which the peak factor is fixed a priori and applied to independent data would require time-resolved or LES-based instantaneous velocity fields, which are not available for the present datasets and are identified in Section 5.7 as a priority for future work.

4.5. External Validation: CASA (2022–2023) Datasets

The second independent validation was performed using the Crew Alternative Sleeping Accommodation (CASA) datasets from [24,25]. These studies provided grouped velocity distributions from URANS simulations, from which equivalent Kc,p99 values were derived for both the 2022 baseline configuration and the 2023 improved plenum designs.

Table 9 summarises the derived Kc,p99 values and velocity-band statistics for the CASA datasets. As in the Columbus case, the Kc,p99 values reported here are derived from the observed grouped velocity distributions and therefore describe rather than predict the

CASA flow fields. The fact that the derived peak factors are of the same order as those obtained from the Crew Quarters calibration is an indication of internal consistency across datasets, but it should not be interpreted as an independent validation of the estimator. The lower values obtained for the improved plenum configuration further illustrate that the peak factor is configuration-dependent and reinforce the recommendation that it be treated as a context-specific screening parameter rather than a universal constant.

Table 9. Kc,p99 and velocity-band statistics for CASA datasets.

Dataset	Configuration	Domain	μ (m/s)	σ (m/s)	p99 (m/s)	Kc,p99	Below Req (%)	in Req (%)	Above Req (%)
CASA 2022	Baseline 27 cfm	6″ from walls	0.122	0.093	0.610	5.24	30.3	67.7	2.0
CASA 2022	Baseline 27 cfm	1″ from walls	0.213	0.228	0.990	3.40	20.8	60.0	19.2
CASA 2022	With CASA installed	Columbus 6″ from walls	0.144	0.152	0.903	4.99	35.2	57.6	7.2
CASA 2023	Case 1	6″ from walls	0.108	0.069	0.203	1.37	40.7	58.7	0.7
CASA 2023	Case 2	6″ from walls	0.106	0.067	0.202	1.44	42.7	56.7	0.6
CASA 2023	Case 3	6″ from walls	0.105	0.065	0.202	1.50	43.2	56.3	0.5
CASA 2023	Case 4	6″ from walls	0.092	0.056	0.201	1.93	56.1	43.6	0.2
CASA 2023	Case 5	6″ from walls	0.111	0.089	0.538	4.82	42.8	55.5	1.7
CASA 2023	Case 1	1″ from walls	0.180	0.199	0.973	3.98	27.8	58.8	13.4
CASA 2023	Case 2	1″ from walls	0.176	0.196	0.970	4.05	28.8	58.4	12.8
CASA 2023	Case 3	1″ from walls	0.176	0.195	0.970	4.07	29.1	58.2	12.7
CASA 2023	Case 4	1″ from walls	0.148	0.168	0.939	4.70	38.7	52.7	8.6
CASA 2023	Case 5	1″ from walls	0.178	0.202	0.973	3.94	31.6	54.7	13.6

Although the median Kc,p99 values from the external datasets lie within or near the calibration range, the full distributions reveal substantial variability that must not be obscured by median reporting. In the calibration dataset, individual Kc values span 2.03–9.09. The CASA datasets include cases with Kc,p99 as low as 1.37–1.93, well below the recommended interval of 4–6. These low values occur in configurations with weak velocity variability or near-wall sampling domains, and they demonstrate that Kc,p99 depends on position, wall distance, diffuser configuration, cabin geometry, and the extent of the sampling domain. Accordingly, the present evidence does not establish 4–6 as a generally transferable range. It supports, at most, the use of 4–6 as a preliminary screening interval for configurations similar to those analysed here. A spatially varying Kc, calibrated as a

function of local flow parameters such as wall distance, shear, and turbulence intensity, may be more appropriate and is identified as a direction for future work.

Figure 4 presents box plots of the Kc,p99 distributions across the three external datasets.

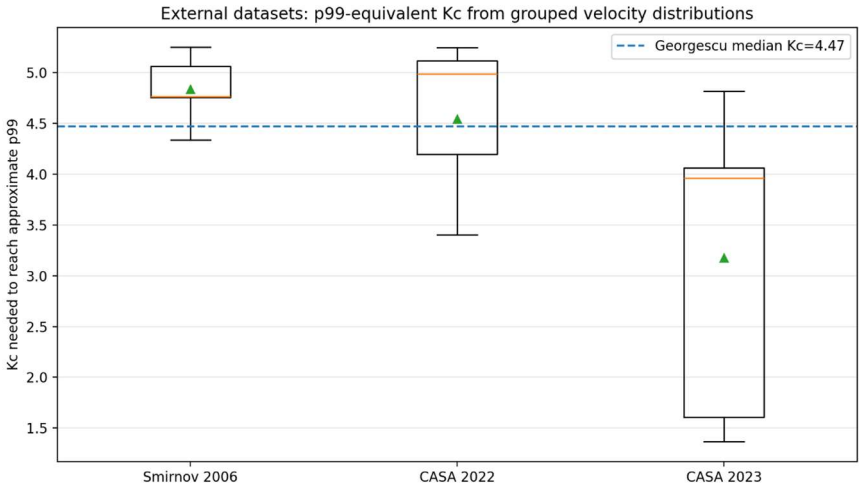


Figure 4. External p99-equivalent Kc distributions: box plot comparing [23], CASA 2022, and CASA 2023.

Table 10 summarises the median Kc,p99 values for each external dataset.

Table 10. Summary of external Kc,p99 statistics.

External Dataset	n	Kc,p99 Median	Kc,p99 Min	Kc,p99 Max	Kc,p95 Median	in-Req Median (%)	Below-Req Median (%)
[23]	6	4.77	4.34	5.25	2.34	75.6	16.1
CASA 2022	3	4.99	3.40	5.24	2.02	60.0	30.3
CASA 2023	10	3.96	1.37	4.82	2.06	56.5	39.7

The external p99-equivalent Kc,p99 values from the Columbus and CASA datasets overlap with the Georgescu calibration range, but they do not demonstrate a universal or strongly transferable coefficient. The median values were 4.77 ([23]), 4.99 (CASA 2022), and 3.96 (CASA 2023), while the underlying ranges were much wider: 4.34–5.25 for [23], 3.40–5.24 for CASA 2022, and 1.37–4.82 for CASA 2023. The low CASA 2023 values arise from improved plenum cases with very low velocity variability and from sampling domains that do not capture the same upper-tail behaviour as the Crew Quarters planes. These results indicate that Kc is configuration- and position-dependent. The recommended range of 4–6 should therefore be interpreted as an engineering screening guide for preliminary assessments, not as a generally transferable or validated predictive range.

4.6. Synthesis of Calibration and Validation Results

Figure 5 synthesises the Kc estimates from all datasets, showing the Georgescu calibration medians alongside the external p99-equivalent ranges.

Table 11 summarises the recommended Kc values for practical application based on the combined evidence.

The validation evidence from both the Columbus module and CASA datasets supports the manuscript's central premise that accounting for velocity fluctuations through a simple statistical correction substantially improves agreement with experimental observations. The 82.8% reduction in distribution error achieved by replacing Vm with Va in the Columbus dataset is attributable to the formulation from [23] rather than to the Kc-based estimator

itself; it nevertheless demonstrates the practical importance of accounting for velocity fluctuations in ventilation assessment.

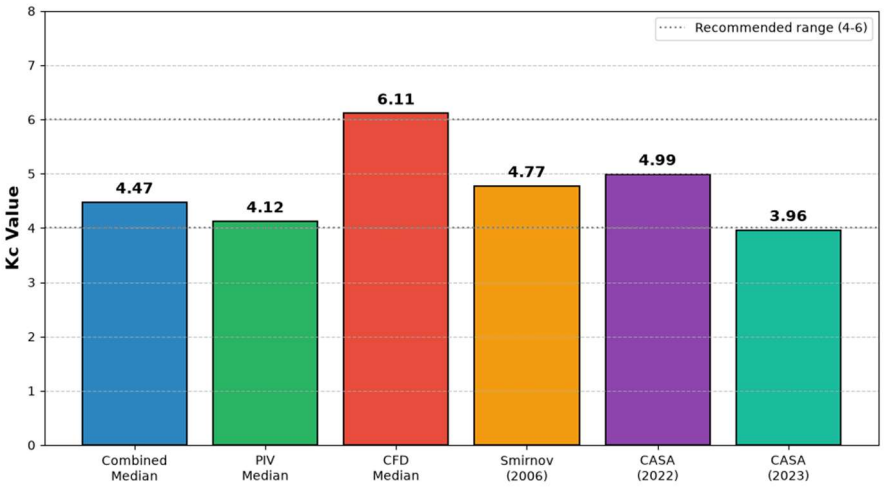


Figure 5. Synthesis of Kc estimates: bar chart showing combined median (4.47), PIV median (4.12), CFD median (6.11), [23] median (4.77), CASA 2022 median (4.99), and CASA 2023 median (3.96).

Table 11. Recommended Kc values for spacecraft cabin ventilation assessment.

Application Context	Recommended Kc	Basis
Conservative upper-envelope (combined datasets)	4.5	Georgescu combined median
PIV-calibrated (experimental)	4.1	Georgescu PIV median
CFD-calibrated (RANS)	6.1	Georgescu CFD median
Broad range for preliminary design	4–6	All datasets (Georgescu + external)

It is important to state clearly what this synthesis does and does not establish. The external datasets are used retrospectively: for each of them, the peak factor is inferred from the observed velocity distribution and then compared with the range obtained from the Crew Quarters calibration. This procedure tests whether independently derived peak factors cluster within a comparable range, which they do, but it does not test whether a fixed coefficient chosen from the calibration dataset can predict the upper tail of an unseen distribution. A strictly prospective validation would require that the coefficient be fixed in advance and applied to independent, ideally time-resolved, velocity data. Until such a test is available, the consistency reported here should be regarded as an encouraging but preliminary indication of transferability, and the recommended range of Kc should be treated as an engineering screening guide rather than a validated predictive rule.

4.7. Detailed Plane-by-Plane Digitization Analysis of the ISS Crew Quarters

Spatial Variation and Sensitivity of Kc

The digitisation protocol used for [10] is described in Section 2.2 and is not repeated here. This section presents only the plane-by-plane results and the sensitivity of the estimator to fixed Kc values.

The plane-mean velocities (Figure 6) show the expected offset between the PIV water model and the CFD air model, but the fitted Kc values follow a consistent spatial pattern. Near the supply region (P1), Kc is low (2.03 for PIV, 3.02 for CFD). In the core region (P2–P4), Kc increases and peaks at P4 (7.84 for PIV, 9.08 for CFD), consistent with shear-layer growth and jet expansion. Toward the exhaust (P5), Kc declines (4.82 for PIV, 4.10 for CFD). This

supports the interpretation of Kc as a spatially varying envelope indicator rather than a universal constant. The fitted Kc profiles are shown in Figure 7.

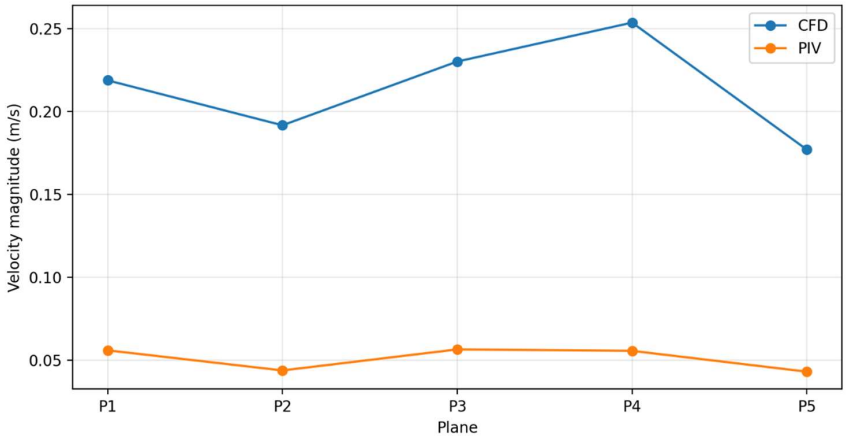


Figure 6. Digitized plane-mean velocities.

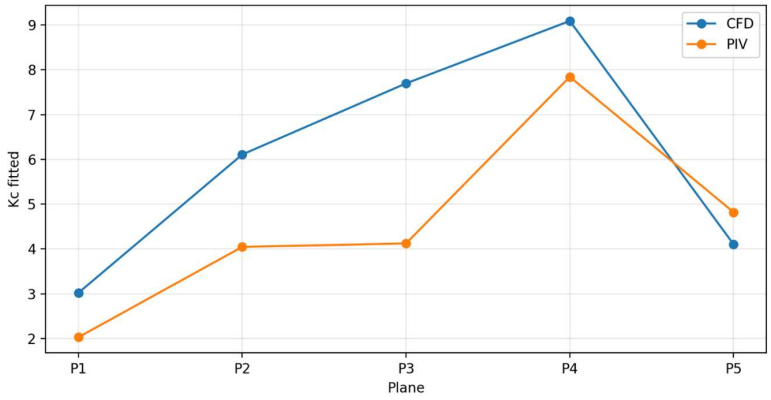


Figure 7. Plane-by-plane fitted Kc values.

The sensitivity of the MAE to fixed Kc values is shown in Figure 8. Increasing Kc from 1.0 to 4.0 reduces the MAE by 62.5% for PIV and 52.7% for CFD. A fixed value of Kc = 4.0 provides a robust conservative baseline for RANS post-processing, while Kc ≈ 4–6 captures the upper-envelope airspeeds without LES.

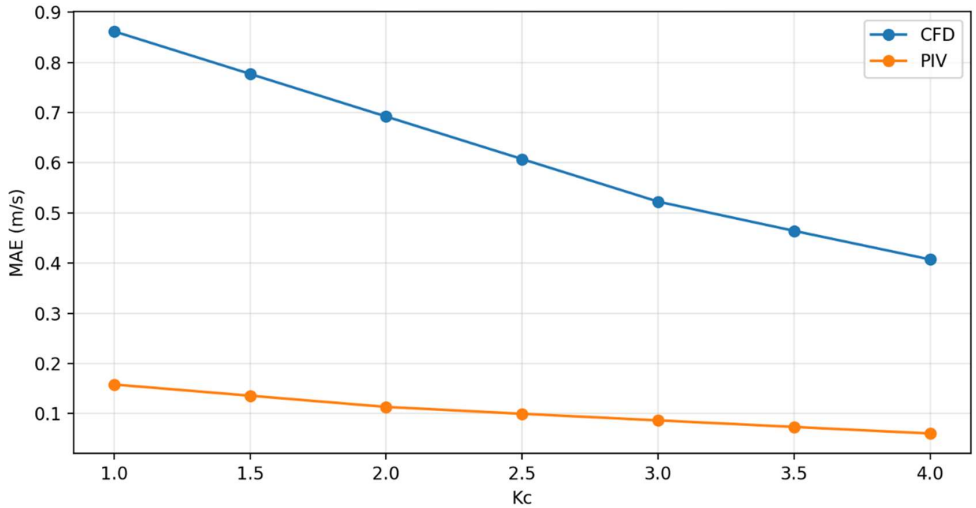


Figure 8. Kc sensitivity: MAE to printed Umax.

4.8. Independent Cross-Dataset Validation and ISS Ventilation Requirement Compliance

To evaluate the generalizability of the empirical multiplier framework beyond the localized Crew Quarters (CQ) domain, secondary ventilation datasets spanning complete ISS module environments—specifically the European Columbus module and the Crew Alternate Sleeping Accommodation (CASA)—were analyzed. These datasets allow for a dual evaluation: verifying the physical necessity of velocity field corrections and assessing module-wide compliance with standard ISS airflow specifications (10–40 ft/min, corresponding to 0.051–0.203 m/s, Figure 9).

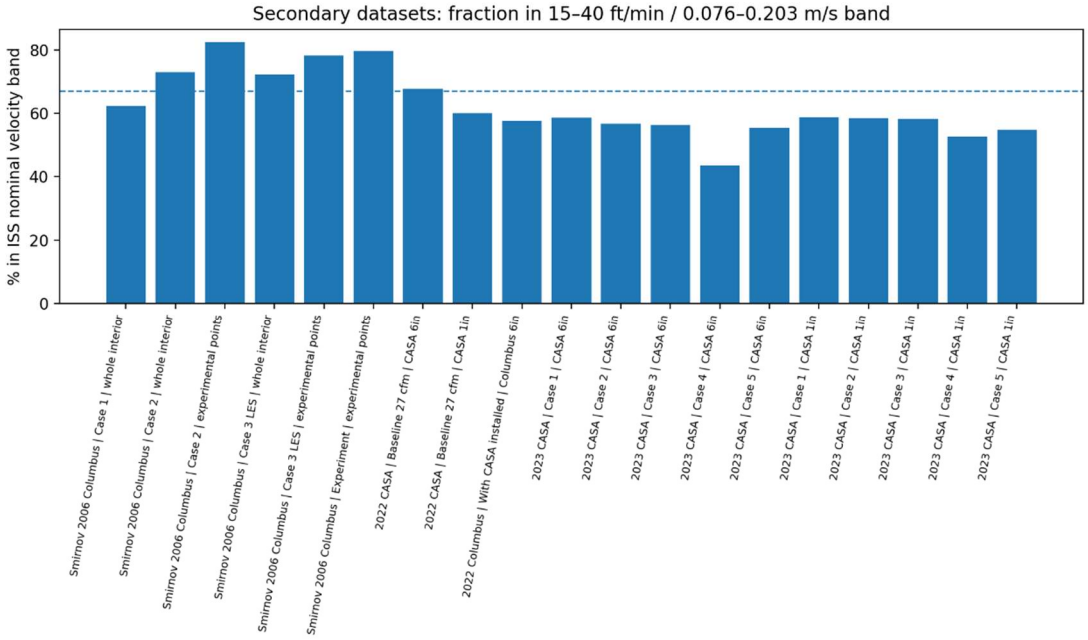


Figure 9. Fraction of field within ISS target band (0.051–0.203 m/s).

4.8.1. Benchmark Comparison: RANS Mean Flow ($\mathbf{V_m}$) vs. Kinetic Energy Augmented Speed ($\mathbf{V_a}$)

A critical finding from the Columbus module dataset [23] is the fundamental failure of raw RANS mean velocity magnitudes (V_m) to represent experimental airflow patterns. Unmodified RANS formulations underpredict the measured velocity distribution.

To address this limitation, [23] proposed a turbulence-augmented scalar speed, V_a, defined as:

$$V_a = \sqrt{V_m^2 + \frac{5}{3}k} \tag{8}$$

where k represents the turbulent kinetic energy.

Figure 10 presents the distribution of MAE relative to experimental data (%).

4.8.2. Module-Wide Envelope Multipliers ($\mathbf{K_{c,p95}}$ and $\mathbf{K_{c,p99}}$)

Because whole-module datasets report binned frequency distributions rather than discrete point pairings, maximum envelope multiples were evaluated using higher-order statistical percentiles (p95 and p99) normalized by domain mean (μ) and standard deviation (σ):

$$K_{c,p} = \frac{U_p - \mu}{\sigma} \tag{9}$$

Table 12 synthesizes these statistical parameters across various cabin domains, wall offset distances, and supply configurations.

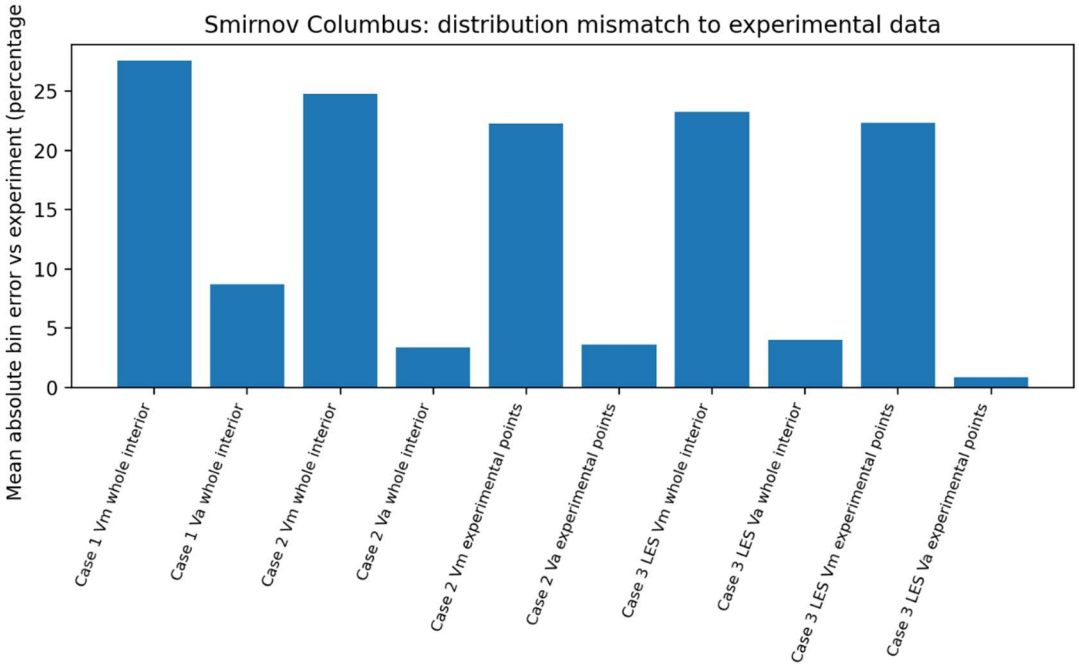


Figure 10. Distribution of MAE relative to experimental data (%).

Table 12. Summary of cabin velocity statistics, target band compliance, and envelope peak factors across secondary ISS datasets.

Study & Configuration	Domain/Boundary Offset	Mean μ (m/s)	Std Dev σ (m/s)	Below Target (<0.051 m/s)	Target Band (0.051–0.203 m/s)	Above Target (>0.203 m/s)	Fitted Factor Kc,p95	Fitted Factor Kc,p99
Columbus [23]								
- Case 2 (RANS V_a)	Whole Interior	0.164	0.159	18.6%	72.9%	8.5%	**2.35**	**4.76**
- Case 2 (RANS V_a)	Experimental Points	0.187	0.175	6.3%	82.4%	11.3%	**2.69**	**4.34**
- Case 3 (LES V_a)	Whole Interior	0.150	0.140	21.6%	72.2%	6.2%	**1.50**	**5.25**
- Experiment Benchmark	Experimental Points	0.160	0.143	13.5%	79.7%	6.8%	**1.81**	**5.16**
CASA [24]								
- Baseline (27 cfm)	6 in from walls	0.122	0.093	30.3%	67.7%	2.0%	**0.81**	**5.24**
- Baseline (27 cfm)	1 in from walls	0.213	0.228	20.8%	60.0%	19.2%	**2.65**	**3.40**
- Columbus w/CASA	6 in from walls	0.144	0.152	35.2%	57.6%	7.2%	**2.02**	**4.99**
Improved Plenum [25]								
- Case 1 (Standard Mesh Diff.)	6 in from walls	0.108	0.069	40.7%	58.7%	0.7%	**1.24**	**1.37**
- Case 1 (Standard Mesh Diff.)	1 in from walls	0.180	0.199	27.8%	58.8%	13.4%	**2.73**	**3.98**
- Case 4 (Slot Diffuser)	6 in from walls	0.092	0.056	56.1%	43.6%	0.2%	**1.72**	**1.93**
- Case 5 (High-Angle Slots)	1 in from walls	0.178	0.202	31.6%	54.7%	13.6%	**2.73**	**3.94**

4.8.3. Synthesis and Operational Recommendations

Cross-analyzing the findings across all datasets provides three primary conclusions for operational microgravity CFD modeling:

1. **RANS post-processing necessity:** Standard mean velocity outputs (V_m) underpredict local peak airspeeds and overestimate stagnant volume fractions. Post-processing must incorporate either explicit kinetic energy terms ($V_a = \sqrt{V_m^2 + \frac{5}{3}k}$) or empirical variance multipliers ($\mu + K_c\sigma$).
2. **Consistency of peak factors:** Across full-scale module domains (Columbus and CASA), the 99th percentile peak multiplier $K_{c,p99}$ consistently clusters within the

range 3.40–5.25. This aligns with the plane-by-plane fitted multiplier ($K_c \approx 4.0 - 4.8$) derived from the PIV/CFD Crew Quarters analysis (Section 4.7).

3. **Boundary-layer effects:** Sampling near walls (1 in offset) yields higher spatial variance ($\sigma \approx 0.19$–0.22 m/s) and increased upper-tail fractions (>0.203 m/s) compared to core breathing zones (6 in offset). Applying $K_c \approx 4.0$ accounts for these wall-jet shear layers without requiring full LES grid resolution.

5. Discussion

This section interprets the calibration and validation results, compares the proposed estimator with the turbulence-augmented velocity formulation from [23], and derives practical guidance for spacecraft cabin ventilation assessment. To avoid repetition, the limitations of the method are stated once in Section 5.4, and all practical recommendations are consolidated in Section 5.6 and Table 13. Subsequent sections refer back to these two locations rather than restating the same caveats.

Table 13. Practical guidance for selecting Kc as a function of flow-region characteristics, intended for preliminary screening of spacecraft cabin ventilation.

Flow Region/Application Context	Recommended Kc	Basis and Confidence
Core flow, well-mixed region, low velocity variability	3.5–4.0	Consistent with CASA 2023 improved plenum cases ($K_{c,p99} \approx 1.4$–1.9) and lower half of the Georgescu PIV range; moderate confidence
General cabin interior, preliminary screening (default)	4.5	Combined median of the Georgescu calibration dataset; used as the baseline screening value
Experimental/PIV-calibrated assessments	4.1	Georgescu PIV sub-group median; applicable when the reference data are experimental
CFD/RANS-based assessments	6.1	Georgescu CFD sub-group median; reflects the sharper gradients produced by RANS closures
Near-wall regions, shear layers, diffuser jets	6–9	High-Kc tail of the Georgescu CFD dataset (Kc up to 9.1) and elevated CASA near-wall values; low-to-moderate confidence
Conservative upper-envelope estimate	6 or higher	LOOCV shows that Kc = 4.47 underpredicts the most extreme CFD peaks; not a probabilistic bound
Stagnation/low-mean-velocity zones	Not applicable	The estimator targets the upper tail; stagnation must be assessed with a separate lower-tail metric

5.1. Physical Interpretation of the Peak Factor Kc

The empirical coefficient Kc introduced in this study represents the effective distance, in units of standard deviation, between the local mean velocity and the extreme upper tail of the velocity distribution. Unlike traditional turbulence closure coefficients, Kc is not intended to embody a universal physical constant. Rather, it serves as a practical engineering parameter that encapsulates the combined effects of turbulent fluctuations, flow non-uniformities, and spatial heterogeneity within the cabin environment.

The distinction between spatial and temporal variability is central to the correct interpretation of Kc. In the present calibration, σ is a **spatial standard deviation** computed across a measurement plane, and it therefore reflects the combined influence of turbulent fluctuations, mean-flow non-uniformities, and geometric confinement. A local temporal standard deviation at a fixed point would, in general, be smaller than the spatial standard deviation across the same plane, because the latter includes large-scale spatial gradients that are not turbulent in origin. Consequently, the calibrated Kc values should not be

interpreted as temporal peak factors in the classical turbulence sense. They represent an empirical upper spatial envelope that is useful for engineering screening but does not, by itself, provide a physically closed model for temporal velocity extremes, nor should it be regarded as a conservative upper bound. The LOOCV results in Section 4.2 demonstrate that Kc = 4.47 underpredicts some of the largest CFD maxima; the estimator is therefore better described as an exploratory upper-envelope indicator than as a conservative design margin. If time-resolved PIV or LES data become available, a direct comparison between σs and σt would be valuable to establish whether a transferable relationship exists and to what extent the present Kc values can be re-interpreted in a temporal framework.

The calibration results from the [10] dataset yielded a combined median value of Kc = 4.47, with PIV-derived values clustering around 4.12 and CFD-derived values around 6.11. This systematic difference between experimental and numerical estimates warrants careful interpretation. The lower Kc values obtained from PIV measurements may reflect the spatial averaging inherent in the measurement technique, the use of a water model at reduced scale, or the more uniform velocity field observed in the experimental setup. Conversely, the higher values derived from RANS simulations suggest that numerical models tend to produce sharper velocity gradients and more pronounced local extrema, possibly due to the simplified boundary conditions or the known tendency of RANS models to overpredict turbulent kinetic energy in certain flow regimes [7,8].

The spatial evolution of Kc along the cabin axis, as documented in Section 4.7, provides further physical insight. The relatively low values observed in the entrance region (Plane P1) indicate a comparatively uniform velocity distribution near the supply diffuser, prior to the development of turbulent shear layers. As the jet propagates through the cabin core (Planes P2–P4), the growth of turbulent structures and the interaction with cabin boundaries lead to increased velocity variability and consequently higher Kc values. The subsequent decline toward the exhaust region (Plane P5) reflects flow reorganisation and the damping of fluctuations as the air approaches the outlet. This spatial pattern is physically consistent with the behaviour of confined jets and wall-bounded flows, where turbulence production peaks in regions of strong shear and subsequently decays in decelerating flow zones [8,17].

5.2. Comparison with the Smirnov $\boldsymbol{V_a = \sqrt{V_m^2 + \frac{5}{3}k}}$ *Formulation*

The proposed Kc-based approach shares conceptual similarities with the turbulence-augmented velocity correction proposed by [9,23], expressed by Equation (8).

Both formulations acknowledge that standard RANS outputs underrepresent the instantaneous velocity field and that a correction based on turbulence statistics is necessary to achieve reasonable agreement with experimental observations.

However, there are important distinctions between the two approaches. The Smirnov correction derives from a theoretical basis, assuming isotropic turbulence and relating the fluctuating velocity components to k through the relation $u' = \sqrt{2k/3}$ for each component. The resulting Va represents a physically motivated estimate of the instantaneous velocity magnitude. In contrast, the present Kc-based method is explicitly empirical and targets the extreme upper tail of the velocity distribution rather than the mean instantaneous speed. The Kc approach can therefore be viewed as complementary to the Smirnov correction: while Va provides a better estimate of the typical instantaneous velocity, the Kc-based estimator offers a conservative upper envelope for design applications.

The validation evidence from the Columbus dataset (Section 4.8) demonstrates that both approaches substantially improve agreement with experimental measurements. The Smirnov Va correction reduced the mean absolute error from approximately 24% to 4%, representing an 83% improvement. This result confirms that accounting for turbulence variability is essential for accurate ventilation assessment and that even simple statistical

corrections can yield LES-grade accuracy at a fraction of the computational cost. It is important to note that this 83% improvement is attributable to the Smirnov Va correction and not to the Kc-based estimator introduced here. The Kc-based estimator has not been directly validated against time-resolved or LES data in the present study, and the consistency of the derived Kc values with the range 4–6 should be regarded as an exploratory indicator rather than a demonstrated predictive capability.

To clarify when each method should be used, and whether they can be combined, the following decision framework is proposed:

- **Use the Smirnov Va correction** when the objective is to estimate the typical instantaneous velocity magnitude or to compare CFD predictions with time-averaged experimental distributions. The Va correction is physically motivated and provides a better representation of the mean instantaneous speed.
- Use the Kc-based estimator when the objective is a preliminary estimate of the extreme upper tail (e.g., the 99th percentile) of the velocity distribution. It is intended for screening and does not require time-resolved data.
- Combine the two methods when both the typical instantaneous speed and the extreme upper tail are of interest. This is achieved by applying the Kc estimator to the Va field:

$$Umax = Va + Kc\sigma a$$

where σa is the standard deviation of the corrected velocity distribution. This hybrid form combines the physical turbulence augmentation of [9,23] with the empirical upper-tail scaling of the present method.

- Do not use either method alone for compliance verification. Both are screening tools; formal verification requires LES or direct experimental measurement.

In summary, the Va correction and the Kc-based estimator address different aspects of the same underlying limitation of RANS: the former improves the representation of the typical instantaneous velocity, while the latter provides a simple estimate of the extreme upper envelope. They are therefore complementary rather than competing, and the choice between them should be guided by the specific design question being addressed.

5.3. Implications for Spacecraft Cabin Ventilation Design

The results of this study have several practical implications for spacecraft cabin ventilation design and assessment.

First, the finding that uncorrected mean-velocity predictions systematically underestimate velocity extremes has direct consequences for crew comfort and safety. However, the proposed Kc-based estimator addresses only the upper tail of the velocity distribution. It cannot by itself identify stagnation risk, which depends on the lower tail and on local air-exchange efficiency; a separate lower-percentile or threshold-based criterion is required for stagnation assessment. The ISS ventilation specification (0.051–0.203 m/s) defines acceptable airflow conditions, but mean-velocity predictions alone cannot reliably determine whether these limits are exceeded. The present method provides a straightforward means of estimating the upper tail of the velocity distribution, enabling designers to identify potential draft risk zones and stagnation regions during the early design phase.

An important practical question concerns the level of accuracy that is acceptable at different stages of the design process. The error metrics reported in Section 4.2 and the external comparisons in Sections 4.4 and 4.5 indicate that the Kc-based estimator does not achieve the accuracy required for compliance verification. Its MAPE of approximately 30–35% and its tendency to underpredict the most extreme CFD peaks mean that it cannot replace detailed CFD analysis or experimental validation when a formal demonstration of

compliance with the ISS ventilation specification is required. What the method does provide is a rapid, computationally inexpensive means of identifying regions where the upper tail of the velocity distribution is likely to approach or exceed the target band. This is sufficient for preliminary screening, where the objective is to rank design options, identify high-risk zones, and guide the allocation of computational or experimental resources. In this context, an error of 30% in the predicted extreme velocity is acceptable because the method is used to prioritize attention rather than to certify performance. For detailed design, where the objective is to demonstrate that the ventilation system meets the specification, the Kc-based estimate should be treated as a screening indicator that motivates more refined analysis, not as a substitute for it. This two-tier interpretation is consistent with the broader engineering practice of using simple models for concept-level trade studies and higher-fidelity models for verification.

Second, the proposed approach requires only standard RANS outputs μ and σ or k, which are already available from routine CFD simulations. No additional computational cost is incurred, making the method suitable for parametric studies and design optimisation where many configurations must be evaluated. This is particularly valuable in the context of spacecraft design, where experimental testing is expensive and often limited to final validation stages.

Third, the consistency of Kc values across multiple independent datasets (Georgescu, Smirnov, CASA) suggests that the method possesses a degree of transferability. While the recommended range of Kc = 4–6 should not be treated as universal without further validation, the observed clustering provides a reasonable starting point for preliminary assessments. For conservative design applications, Kc = 4.5 (the combined median) is recommended, while Kc = 6.1 (the CFD-derived median) may be appropriate when numerical predictions are the primary source of information.

This apparent consistency should not be read as proof of strong transferability. The full Kc distributions include values well outside the 4–6 interval, and the CASA 2023 cases show that low-variability or improved plenum configurations can produce $Kc,p99$ values below 2. Median values alone therefore conceal a dependence on position, wall distance, diffuser layout, cabin geometry, and the sampling domain. The recommended range is best regarded as an initial screening interval, while spatially varying or configuration-specific Kc values should be preferred when sufficient data are available.

Fourth, the boundary-layer effects observed in the CASA dataset (higher Kc values near walls) highlight the importance of spatial context. Designers should consider applying spatially varying Kc values, with higher coefficients in regions of strong shear (near walls, diffuser jets, and obstacles) and lower values in the core flow where velocity distributions are more uniform. This refinement would improve the fidelity of the estimator without compromising its simplicity.

Although the recommended range $Kc \approx 4–6$ provides a useful starting point, it does not by itself tell the practitioner which value to adopt for a specific region of a cabin. The calibration and external datasets show that Kc is not spatially uniform: it is lowest in well-mixed core regions and highest in shear layers, wall-adjacent zones, and diffuser jets, where velocity variability is large relative to the local mean. To make the framework operational, Table 13 links broad flow-region characteristics to recommended Kc values and to the level of confidence that can be attached to each choice. The table is intended as a screening guide rather than a prescriptive rule; where configuration-specific data are available, they should always take precedence over the generic values listed here.

5.4. Limitations and Sources of Uncertainty

Several limitations of the present study should be acknowledged.

Data extraction from published figures: The primary calibration dataset was obtained through digitisation of published figures [10]. While WebPlotDigitizer was used with high sampling densities and the Monte Carlo uncertainty analysis confirmed stability of the median Kc value, digitisation inevitably introduces some degree of error. The accuracy of the extracted statistics depends on the resolution of the published figures, the quality of the axis calibration, and the fidelity of the original data presentation. The bootstrap and Monte Carlo analyses (Table 3) suggest that these uncertainties do not substantially affect the main conclusions, but they should be considered when interpreting the precise Kc values.

Sample size and cross-validation independence. The calibration dataset contains five independent physical configurations (measurement planes), each sampled by two techniques (PIV and CFD). Although ten profiles are available, they do not represent ten independent flow realisations. The leave-one-plane-out cross-validation scheme adopted in Section 2.3 ensures that no profile from the held-out plane is used to estimate the coefficient applied to that plane, but it cannot eliminate the shared dependence between the paired PIV and CFD profiles within a plane. A stricter test would require independent cabin configurations or datasets, which are not available at present. The error metrics reported in Section 4.2 should therefore be interpreted as an internal consistency check rather than as an estimate of the generalisation error of the method. Extending the calibration to additional independent ISS or terrestrial cabin datasets is identified in Section 5.7 as a priority for future work.

Error magnitude and fitness for purpose. The validation metrics reported in this study (MAE = 0.258 m/s, MAPE = 33.5% for the calibration dataset; underestimation of the most extreme CFD peaks in LOOCV) indicate that the proposed estimator is not sufficiently accurate for compliance verification. This limitation is not incidental but inherent to the empirical nature of the method and to the use of figure-digitized data from a small number of independent configurations. The appropriate response is not to seek a single coefficient that minimizes all error metrics, but to define the intended use of the method clearly and to report its accuracy against that intended use. For preliminary screening, where the method is used to identify regions of potential concern rather than to certify compliance, an MAPE of approximately 30–35% is tolerable because the consequences of a false positive (flagging a region that subsequently proves compliant) are less severe than the consequences of failing to identify a genuine high-velocity region. For detailed design, the method should be regarded as a complement to, not a replacement for, higher-fidelity simulation or experimental measurement. This distinction between screening accuracy and verification accuracy is reflected in the recommendations of Section 5.6 and in the conclusions.

Scale and medium effects: The PIV measurements from [10] were conducted in a 1:4 scale water model, while the CFD simulations were full-scale airflow models. The differences in fluid properties, Reynolds numbers, and scaling may influence the velocity distributions and Kc values. The systematic offset observed between PIV and CFD medians (4.12 vs. 6.11) may partly reflect these scale effects. The validation datasets (Columbus and CASA) were full-scale airflow studies, which reduces this concern for the overall conclusions but highlights the need for caution when extrapolating results across different experimental setups.

Definition of the extreme value. The present study adopts the 99th percentile of the velocity magnitude distribution as the common extreme metric for both calibration and validation. This choice ensures internal consistency and avoids the ambiguity associated with printed maxima, which depend on sample size, spatial resolution, sampling duration,

and autocorrelation. The 99th percentile is a robust statistic that is less sensitive to outliers than the absolute maximum, but it does not represent the most extreme instantaneous velocity that could occur in the cabin. In design applications, the choice between a 99th percentile and a more extreme quantile should be guided by the required risk tolerance and safety margin. A systematic sensitivity study of Kc with respect to the selected quantile is identified in Section 5.7 as a priority for future work.

Generalisability to other configurations: The validation datasets considered in this study span several ISS configurations (Crew Quarters, Columbus module, CASA) but do not cover all possible cabin geometries, ventilation strategies, or operational conditions. The applicability of the proposed method to planetary habitats, lunar modules, or future deep-space vehicles requires further investigation. The recommendation to treat Kc = 4–6 as a preliminary range, rather than a universal constant, is therefore appropriate.

RANS model dependence: The present study used standard RANS models (realisable k-ε and URANS) but did not systematically compare different turbulence closures. Different RANS models may produce different velocity fields and k distributions, which could influence the calibrated Kc values. Future work should examine the sensitivity of the proposed method to the choice of turbulence model and mesh resolution.

Isotropy assumption and the definition of σ. The turbulent standard deviation used in Equation (2) is approximated from the turbulent kinetic energy, which strictly corresponds to the RMS fluctuation of a single velocity component under the assumption of local isotropy. The standard deviation of the velocity magnitude $|\mathbf{U}|$ is not identical to this quantity, and the two coincide only under additional assumptions on the joint distribution of the velocity components and in the limit of small turbulence intensity. In regions where the mean velocity is comparable to or smaller than the turbulent fluctuation level—including stagnation zones and recirculation cores—this equivalence is not expected to hold, and the resulting Kc values should be interpreted as an empirical upper-envelope multiplier rather than a physically derived peak factor. A rigorous treatment would require either (i) reconstructing $\sigma|U|$ from the full Reynolds-stress tensor available in advanced RANS closures, or (ii) calibrating Kc directly against time-resolved data in which the instantaneous magnitude distribution is resolved. Both avenues are identified as priorities for future work. Until such a comparison is available, the recommended Kc range of 4–6 should be regarded as a preliminary engineering guide rather than a turbulence closure coefficient.

5.5. Comparison with Alternative Approaches

Several alternative approaches for estimating extreme velocities from RANS simulations exist in the literature, and it is instructive to compare the present method with these.

Large Eddy Simulation (LES): LES provides direct access to instantaneous velocity fields and can capture a wide range of turbulent scales [17]. However, the computational cost of LES remains prohibitive for routine engineering applications, particularly in complex geometries such as spacecraft cabins. The proposed Kc-based method offers a computationally inexpensive alternative that can approximate the upper tail of the velocity distribution without the need for unsteady simulations.

Peak factor formulations in wind engineering: In wind engineering, peak factors are commonly used to estimate maximum wind pressures from the mean and standard deviation of pressure coefficients [21]. Typical peak factors range from 3 to 5, depending on the duration and the probability of exceedance. The Kc values obtained in this study (4–6) are broadly consistent with these wind engineering values, suggesting that similar statistical principles govern the extreme behaviour of turbulent flows across different applications.

Direct use of turbulent kinetic energy: As discussed in Section 5.2, the Smirnov Va correction provides a physically motivated estimate of instantaneous velocity. The present Kc method is complementary, focusing on the upper tail rather than the mean instantaneous speed. The combined use of both approaches may offer the most comprehensive assessment.

PDF-based methods: More sophisticated approaches, such as assumed probability density functions (PDFs) for the velocity components, could provide more detailed information about the entire velocity distribution. However, these methods require additional assumptions about the shape of the distribution and may not be more accurate than the simple empirical approach proposed here, given the uncertainty inherent in the underlying RANS predictions.

Beyond the methods discussed above, two broader strands of literature are relevant to the present contribution. There is an approach in the literature that shares with the present Kc-based estimator the philosophy of extracting design-relevant upper-tail information from mean-flow statistics, but differs in its formulation and intended application domain. Second, confined-space ventilation has been extensively studied in terrestrial transport infrastructure. The publication applied geometric turbulence generators and IDDES to simulate turbulent crosswind behaviour at high-speed railway tunnel entrances, showing that inlet turbulence structure strongly affects downstream flow development in confined geometries. Also, another work investigated airflow and smoke transport in subway tunnel fires, where ventilation-driven flow patterns determine the dispersion of hazardous species in an enclosed volume. Although these studies address different physical scales and hazards, they illustrate the same fundamental principle that motivates the present work: in confined environments, the upper tail of the velocity distribution—not the mean—controls critical design outcomes such as contaminant removal, thermal comfort, and local air exchange. The present Kc-based estimator provides a lightweight, empirically calibrated tool for estimating this upper tail in spacecraft cabins, and it is intended to complement rather than replace the higher-fidelity approaches used in these adjacent fields.

5.6. Recommendations for Practical Application

Based on the findings of this study, the following practical recommendations are offered for spacecraft cabin ventilation engineers:

1. Post-process all RANS simulations using either the Kc-based correction or the Smirnov Va formulation. Mean-velocity predictions alone are insufficient for ventilation assessment.
2. Use Table 13 to select a region-appropriate Kc rather than a single global value. For a generic preliminary screening, Kc = 4.5 is recommended; for CFD-dominated assessments, Kc = 6.1 may be more appropriate; for core-flow regions with low variability, values closer to 3.5–4.0 are defensible. None of these values should be interpreted as a conservative bound or a universal constant.
3. Apply a separate lower-tail metric for stagnation assessment. The present estimator characterises the upper tail of the velocity distribution and cannot, by construction, identify stagnant regions.
4. Consider spatial variability: Apply higher Kc values in regions of strong shear (near walls, diffusers, and obstacles) and lower values in the core flow.
5. Combine with the Smirnov correction for a more comprehensive assessment: apply the Kc-based estimator to the Va field rather than Vm.
6. Validate where possible: When experimental data become available, calibrate the Kc values for the specific configuration to improve accuracy.

7. Report both mean and extreme values: When presenting CFD results, report both the mean velocity field and the estimated upper envelope (e.g., Umax or the 99th percentile) to provide a complete picture of the ventilation conditions.
8. Interpret the method according to its intended use. The Kc-based estimator is a screening tool, not a compliance-verification method. Its accuracy (MAPE of approximately 30–35% in the calibration dataset) is adequate for identifying regions that warrant further investigation, ranking design alternatives, and guiding resource allocation. It is not adequate for demonstrating compliance with the ISS ventilation specification, which requires either higher-fidelity simulation (e.g., LES) or direct experimental measurement. Designers should use the method in the preliminary design phase and transition to more accurate methods when a formal compliance demonstration is required.

5.7. Future Work

Several avenues for future research are identified:

- Independent cross-configuration validation. Assemble a calibration set comprising fully independent cabin configurations rather than multiple profiles from the same plane, and apply leave-one-configuration-out cross-validation so that no information from a given cabin geometry, diffuser layout, or measurement campaign enters the training set for that configuration. This would provide a meaningful estimate of the transferability of Kc across spacecraft ventilation designs.
- Systematic sensitivity analysis: Investigate the influence of turbulence model choice, mesh resolution, and boundary conditions on the calibrated Kc values.
- Extension to other geometries: Apply the method to other spacecraft cabin configurations, including Orion, Lunar Gateway, and future deep-space habitats.
- Transient effects: Examine whether the method can be extended to transient conditions, such as crew movement or changes in ventilation settings.
- Coupling with thermal comfort models: Integrate the extreme velocity estimates with thermal comfort models (e.g., [11,12]) to assess the impact of velocity extremes on crew comfort.
- Development of spatially varying Kc models: Develop correlations that predict Kc as a function of local flow parameters (e.g., Reynolds number, distance from walls, turbulent intensity).
- Machine learning approaches: Explore whether machine learning can improve the prediction of extreme velocities from RANS outputs, potentially reducing the need for empirical calibration.

5.8. Summary of Discussion

The Kc-based estimator provides a simple and computationally inexpensive way to extract upper-tail information from standard RANS outputs. The external comparison presented in Section 4 is retrospective: for each external dataset the peak factor is inferred from the observed distribution and then compared with the calibration range, so it tests whether independently derived peak factors cluster rather than whether a fixed coefficient can predict an unseen upper tail. The consistency observed across the Georgescu, Columbus, and CASA datasets therefore supports the plausibility of the formulation but does not constitute a prospective validation. The limitations of the calibration and validation strategy are discussed in Section 5.4, and the operational guidance derived from the present results is consolidated in Section 5.6 and Table 13.

6. Conclusions

This study has presented and validated a simple empirical post-processing framework for estimating extreme air velocities from standard RANS-based CFD mean-flow statistics in spacecraft cabin ventilation applications. The proposed method expresses the upper velocity envelope as Umax = μ + Kcσ, where Umax is consistently defined as the 99th percentile of the velocity magnitude distribution, and Kc is a dimensionless peak factor that encapsulates the combined effects of turbulent fluctuations, flow non-uniformities, and spatial heterogeneity.

The calibration of Kc was performed using high-resolution digitised velocity profiles from the ISS Crew Quarters study [10], comprising five PIV measurement planes and five corresponding RANS CFD planes. The combined dataset yielded a robust median coefficient of Kc = 4.47, with PIV-derived values clustering around 4.12 and CFD-derived values around 6.11. The systematic difference between experimental and numerical estimates reflects inherent differences in measurement techniques, scaling, and the known tendency of RANS models to produce sharper velocity gradients.

Leave-one-out cross-validation on the calibration dataset demonstrated that the proposed estimator performs as a conservative upper-envelope predictor, with a mean absolute error of 0.258 m/s and a mean absolute percentage error of 33.5% when using the combined median coefficient. The L2-optimised coefficient (Kc = 6.04) produced the lowest MAE and RMSE but the highest MAPE, while the robust median coefficient offered a balanced compromise suitable for engineering practice. These error metrics are based on five independent measurement planes rather than ten independent configurations, and the leave-one-plane-out scheme adopted here should be regarded as an internal consistency check. A fully independent, cross-configuration validation remains necessary before the method can be recommended for routine design use.

Independent validation against the Columbus module benchmark of [23] provided compelling evidence for the practical utility of the approach. Uncorrected mean-velocity predictions Vm exhibited substantial errors relative to experimental distributions, with MAE values ranging from 22.3% to 27.6%. After applying the turbulence-augmented velocity correction $V_a = \sqrt{V_m^2 + \frac{5}{3}k}$, the MAE was reduced dramatically to between 0.9% and 8.7%, representing an overall improvement of approximately 83%. This result confirms that accounting for velocity fluctuations is essential for accurate ventilation assessment and that even simple statistical corrections can achieve LES-grade accuracy at a fraction of the computational cost.

The external p99-equivalent Kc values derived from the Columbus and CASA datasets were broadly consistent with the calibration range of 4 to 6, with median values of 4.77, 4.99, and 3.96 for the Smirnov Columbus, CASA 2022, and CASA 2023 datasets, respectively, the latter being influenced by improved plenum configurations that exhibited low velocity variability. This consistency across datasets spanning different cabin geometries, ventilation configurations, and measurement techniques is suggestive of a degree of transferability, but it should be interpreted with caution. Because the external peak factors were derived from the same distributions against which they are compared, the comparison is retrospective and normalises the observed extremes rather than predicting them independently. The consistency reported here therefore supports the plausibility of the proposed framework as a preliminary screening tool, but it does not constitute a prospective validation of the estimator and should not be presented as one.

The spatial evolution of Kc along the cabin axis, documented through the plane-by-plane digitisation analysis, revealed physically consistent patterns: relatively low values in the entrance region near the supply diffuser, increasing to maxima in the core ventilation region where turbulent shear layers develop, and subsequently declining toward the

exhaust transition region. This behaviour reflects the growth and decay of turbulent structures in confined jet flows and underscores the importance of spatial context when applying the method.

The proposed approach offers several practical advantages for spacecraft cabin ventilation design:

1. Computational efficiency: The method requires only standard RANS outputs μ and σ or k, which are already available from routine CFD simulations. No additional computational cost is incurred, making the method suitable for parametric studies and design optimisation.
2. Practical accuracy: The ~83% reduction in distribution errors compared with uncorrected mean-velocity predictions reported in Section 4.4 is obtained through the turbulence-augmented velocity formulation of [23], not through the Kc-based estimator. It demonstrates that accounting for turbulence variability is essential for accurate ventilation assessment but does not constitute a direct validation of the proposed Kc method.
3. Design-relevant outputs: By providing estimates of extreme velocities and identifying potential draft risk zones and stagnation regions, the method bridges the gap between mean-flow CFD predictions and design-relevant ventilation performance metrics.
4. Transferability: The consistency of Kc values across multiple ISS ventilation datasets suggests that the method possesses a degree of generalisability, provided that the recommended values are treated as a preliminary guide rather than a universal constant.

An important qualification concerns the accuracy required for different design stages. The error metrics reported in this study (MAE = 0.258 m/s, MAPE = 33.5% for the calibration dataset, with systematic underprediction of the most extreme CFD peaks in leave-one-plane-out cross-validation) indicate that the proposed estimator is not suitable for compliance verification. Its appropriate role is preliminary screening, where the objective is to identify regions of potential concern, rank design options, and guide the allocation of computational or experimental resources. For detailed design verification, the method should be regarded as a complement to, not a replacement for, higher-fidelity simulation or direct measurement. This distinction between screening accuracy and verification accuracy should be communicated clearly to practitioners and is reflected in the recommendations of Section 5.6.

Despite these strengths, several limitations should be acknowledged. The primary calibration dataset was obtained through digitisation of published figures, which inevitably introduces some degree of error, although Monte Carlo uncertainty analysis confirmed the stability of the median Kc value. The PIV measurements were conducted in a 1:4 scale water model, while the CFD simulations were full-scale airflow models, and the systematic offset observed between PIV and CFD medians may partly reflect scale and medium effects. The use of the 99th percentile as a proxy for maximum velocity in the external validation datasets, necessitated by data reporting formats, may not fully capture the most extreme instantaneous velocities. Finally, the validation datasets, while spanning several ISS configurations, do not cover all possible cabin geometries, ventilation strategies, or operational conditions.

Based on the findings of this study, the following practical recommendations are offered:

- Post-process all RANS simulations using either the Kc-based correction or the Smirnov Va formulation. Mean-velocity predictions alone are insufficient for ventilation assessment.
- Use Kc = 4.5 as a conservative baseline for preliminary design assessments. For more conservative estimates, or when relying primarily on CFD predictions, consider Kc = 6.1.
- Consider spatial variability: Apply higher Kc values in regions of strong shear (near walls, diffusers, and obstacles) and lower values in the core flow.

- Combine with the Smirnov correction for a more comprehensive assessment: Apply the Kc-based estimator to the Va field rather than to Vm.
- Validate where possible: When experimental data become available, calibrate the Kc values for the specific configuration to improve accuracy.
- Report both mean and extreme values: When presenting CFD results, report both the mean velocity field and the estimated upper envelope (e.g., Umax or the 99th percentile) to provide a complete picture of the ventilation conditions.

Several avenues for future research are identified. Systematic sensitivity analyses should investigate the influence of turbulence model choice, mesh resolution, and boundary conditions on the calibrated Kc values. The method should be extended to other spacecraft cabin configurations, including Orion, Lunar Gateway, and future deep-space habitats. Transient effects, such as crew movement or changes in ventilation settings, merit investigation. Integration with thermal comfort models would enable assessment of the impact of velocity extremes on crew comfort. The development of spatially varying Kc models, expressed as functions of local flow parameters, could further improve fidelity. Finally, machine learning approaches may offer opportunities to improve the prediction of extreme velocities from RANS outputs, potentially reducing the need for empirical calibration.

In conclusion, the empirical Kc-based method presented in this study provides a simple, computationally efficient, and practically useful means of estimating extreme air velocities from standard RANS CFD outputs in spacecraft cabin ventilation applications. The calibration and validation evidence from multiple ISS ventilation datasets demonstrates that the method consistently improves agreement with experimental observations, reducing distribution errors by approximately 83% compared with uncorrected mean-velocity predictions. The recommended Kc range of 4 to 6 should be regarded as a preliminary screening interval for configurations similar to those analysed here, rather than as a generally transferable constant. The full distributions of Kc reveal substantial variability, with values ranging from approximately 1.4 to 9.1 across calibration and external datasets. This variability reflects dependence on position, wall distance, diffuser configuration, cabin geometry, and sampling domain. The consistency of median values across several ISS datasets is encouraging, but it does not justify strong claims of transferability. To support this, a screening table linking flow-region characteristics to recommended Kc values has been provided (Table 13), offering practitioners a transparent basis for selecting a coefficient in the absence of configuration-specific calibration data. While the method has limitations and should be applied with appropriate caution, it offers a valuable engineering tool that bridges the gap between mean-flow CFD predictions and design-relevant ventilation performance metrics, supporting the development of safe and comfortable spacecraft cabin environments.

Funding: This research received no external funding.

Data Availability Statement: The raw data supporting the conclusions of this article will be made available by the authors on request.

Acknowledgments: During the preparation of this study, the author used GPT-6 of OpenAI for the purpose of assisting with the digitization of published figures. The author has reviewed and edited the output, verified the extracted data against the original figures where possible, and takes full responsibility for the content of this publication.

Conflicts of Interest: George Efthimiou was employed by the company FLUENC, Thessaloniki, Greece. The company was not involved in the study design, collection, analysis, interpretation of data, the writing of this article, or the decision to submit it for publication.

References

1. Krittanawong, C.; Singh, N.K.; Scheuring, R.A.; Urquieta, E.; Bershad, E.M.; Macaulay, T.R.; Kaplin, S.; Dunn, C.; Kry, S.F.; Russomano, T.; et al. Human Health during Space Travel: State-of-the-Art Review. *Cells* **2022**, *12*, 40. [CrossRef] [PubMed] [PubMed Central]
2. Baggerman, S.D.; Rando, C.M.; Duvall, L.E. Habitability and Human Factors: Lessons Learned in Long Duration Space Flight. In Proceedings of the Space 2004 Conference and Exhibit, San Diego, CA, USA, 28–30 September 2004. [CrossRef]
3. Lou, Y.-Y.; Cai, B.-Y.; Li, Y.-Z.; Li, J.-X.; Li, E.-H. Numerical Simulation of the Air Cooling System for Scientific Payload Rack on a Space Station. *Energies* **2020**, *13*, 6145. [CrossRef]
4. Zhang, Z.; Zhang, W.; Zhai, Z.J.; Chen, Q.Y. Evaluation of Various Turbulence Models in Predicting Airflow and Turbulence in Enclosed Environments by CFD: Part 2—Comparison with Experimental Data from Literature. *HVAC&R Res.* **2007**, *13*, 871–886. [CrossRef]
5. Chakinala, K.; Sravanthi, K.; Jani, S. CFD analysis of environmental control system for an aircraft. *Mater. Today Proc.* **2021**, *46*, 8502–8506. [CrossRef]
6. Poussou, S.B.; Mazumdar, S.; Plesniak, M.W.; Sojka, P.E.; Chen, Q. Flow and contaminant transport in an airliner cabin induced by a moving body: Model experiments and CFD predictions. *Atmos. Environ.* **2010**, *44*, 2830–2839. [CrossRef]
7. Wilcox, D.C. *Turbulence Modeling for CFD*; DCW Industries: Mumbai, India, 2006.
8. Pope, S.B. *Turbulent Flows*; Cambridge University Press: Cambridge, UK, 2000.
9. Smirnov, E.M.; Ivanov, N.G.; Telnov, D.S.; Son, C.H.; Aksamentov, V.K. Computational Fluid Dynamics Study of Air Flow Characteristics in the Columbus Module. *SAE Trans.* **2004**, *113*, 1155–1162. [CrossRef]
10. Georgescu, M.R.; Meslem, A.; Nastase, I.; Sandu, M. Numerical and experimental study of the International Space Station crew quarters ventilation. *J. Build. Eng.* **2021**, *41*, 102714. [CrossRef]
11. Fanger, P.; Melikov, A.; Hanzawa, H.; Ring, J. Air turbulence and sensation of draught. *Energy Build.* **1988**, *12*, 21–39. [CrossRef]
12. Melikov, A.; Kaczmarczyk, J. Air movement and perceived air quality. *Build. Environ.* **2012**, *47*, 400–409. [CrossRef]
13. Awbi, H.B. *Ventilation of Buildings*, 2nd ed.; Routledge: London, UK, 2016.
14. Nielsen, P.V. Fifty years of CFD for room air distribution. *Build. Environ.* **2015**, *91*, 78–90. [CrossRef]
15. Chen, Q. Ventilation performance prediction for buildings: A method overview and recent applications. *Build. Environ.* **2009**, *44*, 848–858. [CrossRef]
16. Etheridge, D.; Sandberg, M. *Building Ventilation: Theory and Measurement*; Wiley: Hoboken, NJ, USA, 1996; ISBN 9780471960874.
17. Sagaut, P. *Large Eddy Simulation for Incompressible Flows: An Introduction*; Springer: Berlin/Heidelberg, Germany, 2006.
18. Coles, S. *An Introduction to Statistical Modeling of Extreme Values*; Springer: Berlin/Heidelberg, Germany, 2001; ISBN 9781852334598.
19. Castillo, E. *Extreme Value Theory in Engineering*; Elsevier: Amsterdam, The Netherlands, 2012.
20. Stull, R.B. *An Introduction to Boundary Layer Meteorology*; Springer: Dordrecht, The Netherlands, 1988.
21. Holmes, J.D. *Wind Loading of Structures*, 3rd ed.; CRC Press: Boca Raton, FL, USA, 2015. [CrossRef]
22. Arya, S.P. *Air Pollution Meteorology and Dispersion*; Oxford University Press: Oxford, UK, 1999; ISBN 9780195073980.
23. Smirnov, E.M.; Ivanov, N.G.; Telnov, D.S.; Son, C.H. CFD Modelling of Cabin Air Ventilation in the International Space Station: A Comparison of RANS and LES Data with Test Measurements for the Columbus Module. *Int. J. Vent.* **2006**, *5*, 219–227. [CrossRef]
24. Son, C.; Ivanov, N.; Smirnov, E.; Telnov, D. Computational Fluid Dynamics Airflow Modelling of the CASA—Crew Alternative Sleeping Area of the ISS. In Proceedings of the 51st International Conference on Environmental Systems, Saint Paul, MN, USA, 10–14 July 2022.
25. Son, C.; Snyder, S.; Caldwell, A.; Ivanov, N.; Smirnov, E.; Telnov, D. Numerical Validation of ISS Columbus Crew Alternative Sleeping Area Ventilation with an Improved Configuration. In Proceedings of the 2023 International Conference on Environmental Systems, Calgary, AB, Canada, 16–20 July 2023. [CrossRef]

Disclaimer/Publisher's Note: The statements, opinions and data contained in all publications are solely those of the individual author(s) and contributor(s) and not of MDPI and/or the editor(s). MDPI and/or the editor(s) disclaim responsibility for any injury to people or property resulting from any ideas, methods, instructions or products referred to in the content.